MCB
Journals.ASM.org

Overexpression of the Insulin-Like Growth Factor II Receptor Increases β-Amyloid Production and Affects Cell Viability

Y. Wang,[a,b] V. Buggia-Prévot,[c] M. E. Zavorka,[d] R. C. Bleackley,[e] R. G. MacDonald,[d] G. Thinakaran,[c] S. Kar[a,b,f]

Departments of Psychiatry,[a] Biochemistry,[e] and Medicine[f] and Centre for Prions and Protein Folding Diseases,[b] University of Alberta, Edmonton, Alberta, Canada; Departments of Neurobiology, Neurology, and Pathology, The University of Chicago, Chicago, Illinois, USA[c]; Department of Biochemistry and Molecular Biology, University of Nebraska Medical Center, Omaha, Nebraska, USA[d]

Amyloid β (Aβ) peptides originating from amyloid precursor protein (APP) in the endosomal-lysosomal compartments play a critical role in the development of Alzheimer's disease (AD), the most common type of senile dementia affecting the elderly. Since insulin-like growth factor II (IGF-II) receptors facilitate the delivery of nascent lysosomal enzymes from the *trans*-Golgi network to endosomes, we evaluated their role in APP metabolism and cell viability using mouse fibroblast MS cells deficient in the murine IGF-II receptor and corresponding MS9II cells overexpressing the human IGF-II receptors. Our results show that IGF-II receptor overexpression increases the protein levels of APP. This is accompanied by an increase of β-site APP-cleaving enzyme 1 levels and an increase of β- and γ-secretase enzyme activities, leading to enhanced Aβ production. At the cellular level, IGF-II receptor overexpression causes localization of APP in perinuclear tubular structures, an increase of lipid raft components, and increased lipid raft partitioning of APP. Finally, MS9II cells are more susceptible to staurosporine-induced cytotoxicity, which can be attenuated by β-secretase inhibitor. Together, these results highlight the potential contribution of IGF-II receptor to AD pathology not only by regulating expression/processing of APP but also by its role in cellular vulnerability.

Alzheimer's disease (AD) is a progressive neurodegenerative disorder characterized by severe memory loss followed by the deterioration of higher cognitive functions. Although most cases of AD occur sporadically after the age of 60 years, a small proportion of cases correspond to the early-onset (<60 years) autosomal dominant form of the disease. To date, mutations in three genes, the amyloid precursor protein (*APP*) gene on chromosome 21, the presenilin 1 (*PSEN1*) gene on chromosome 14, and the presenilin 2 (*PSEN2*) gene on chromosome 1, have been identified as the cause of a large proportion of early-onset familial AD (1–3). Additionally, inheritance of the ε4 allele of the apolipoprotein E (*APOE*) gene on chromosome 19 increases the risk of late-onset and sporadic AD. The neuropathological features associated with AD include the presence of extracellular β-amyloid (Aβ) peptide-containing neuritic plaques, intracellular tau-positive neurofibrillary tangles, and the loss of synapses and neurons in defined brain regions. Several lines of *in vivo* evidence suggest that Aβ peptides initiate or contribute to the neuronal loss and development of AD pathology (2, 4). Aβ peptides are generated from APP, a type I transmembrane protein, which can be processed either by nonamyloidogenic α-secretase or amyloidogenic β-secretase pathways (5, 6). The α-secretase cleaves APP within the Aβ domain, yielding soluble APPα and a 10-kDa C-terminal fragment (CTF-α), which then can be processed by γ-secretase to generate $Aβ_{17–40}$/$Aβ_{17–42}$ fragments. The β-secretase, on the other hand, cleaves APP to generate soluble APPβ and an Aβ-containing C-terminal fragment (CTF-β), which is further processed via γ-secretase to yield full-length $Aβ_{1–40}$/$Aβ_{1–42}$ peptides. While α-secretase processing occurs mostly in the secretory pathway, the endosomal-lysosomal (EL) system plays a critical role in the production of Aβ peptides (5, 6).

The insulin-like growth factor II/cation-independent mannose 6-phosphate (IGF-II/CIM6P or IGF-II) receptor is a 250-kDa multifunctional glycoprotein that recognizes, via distinct sites, two different classes of ligands: (i) M6P-containing molecules, such as lysosomal enzymes, and (ii) IGF-II, a mitogenic polypeptide with structural homology to IGF-I and insulin (7–9). A subpopulation of the receptor located on the plasma membrane regulates internalization of IGF-II and various M6P-containing ligands for their subsequent clearance or activation. There is also evidence that the surface IGF-II receptor can mediate intracellular signaling in response to IGF-II binding (9–11). The majority of the receptors, however, localize within the EL system and function in the recognition of newly synthesized lysosomal enzymes in the *trans*-Golgi network (TGN) for sorting and delivery to endosomes/lysosomes. Several studies have shown that the IGF-II receptor is expressed in many tissues, including the brain, and its expression is known to be altered in response to ischemic, electrolytic, or chemical brain trauma, suggesting a role for the receptor in degenerative and/or regenerative processes (12–20). Since the EL system, the major site of steady-state IGF-II receptor localization, is critical in the generation of Aβ peptides (5, 21, 22), it is likely that the receptor has a role in AD pathology. This is partly supported by evidence that (i) the IGF-II receptor is present in a subset of Aβ-containing neuritic plaques and tau-positive neurofibrillar tangles in the AD brain (23), and (ii) the receptor levels are altered in affected regions of the AD brain in individuals with

Received 4 November 2014 **Returned for modification** 2 December 2014
Accepted 20 April 2015

Accepted manuscript posted online 4 May 2015

Citation Wang Y, Buggia-Prévot V, Zavorka ME, Bleackley RC, MacDonald RG, Thinakaran G, Kar S. 2015. Overexpression of the insulin-like growth factor II receptor increases β-amyloid production and affects cell viability. Mol Cell Biol 35:2368–2384. doi:10.1128/MCB.01338-14.

Address correspondence to S. Kar, skar@ualberta.ca.

doi:10.1128/MCB.01338-14

TABLE 1 Details of the primary antibodies used in this study

Antibody	Type	Dilution for[a]: IF	WB	Source
ADAM10	Polyclonal	NA	1:1,000	EMD Millipore
APP, clone 22C11	Monoclonal	1:2,000	1:2,000	EMD Millipore
APP, clone Y188	Monoclonal	NA	1:2,000	Abcam
APLP1	Polyclonal	NA	1:2,000	Our laboratory
APH-1	Polyclonal	NA	1:500	EMD Millipore
Calnexin	Polyclonal	1:200	NA	Santa Cruz Biotechnology
Caveolin 1	Monoclonal	NA	1:1,000	BD Transduction Laboratories
GFP	Monoclonal	NA	1:800	Roche
IDE	Polyclonal	NA	1:1,000	Abcam
IGF-II receptor	Polyclonal	1:3,000	1:3,000	Gift from C. Scott
IGF-II receptor	Monoclonal	NA	1:4,000	Abcam
LAMP1	Polyclonal	1:200	NA	Santa Cruz Biotechnology
Neprilysin	Polyclonal	NA	1:200	Our laboratory
PKCα	Polyclonal	NA	1:1,000	EMD Millipore
PS1	Monoclonal	1:1,000	1:1,000	EMD Millipore
Rab11	Polyclonal	1:200	NA	Abcam
Rab5	Polyclonal	1:200	NA	Santa Cruz Biotechnology
Rab7	Polyclonal	1:200	NA	Santa Cruz Biotechnology
Transferrin receptor	Polyclonal	NA	1:1,000	BD Transduction Laboratories
β-Actin	Monoclonal	NA	1:5,000	Sigma-Aldrich
BACE1	Monoclonal	1:2,000	1:2,000	R&D Systems

[a] IF, immunofluorescence; WB, Western blotting; NA, not used in that specific application.

PSEN1 mutations or those carrying *APOE* ε4 alleles (23, 24). Additionally, IGF-II receptor levels are markedly increased along with lysosomal enzymes in a line of mutant APP transgenic mice overproducing Aβ peptides (25). However, it remains unclear whether the receptor can directly influence the generation of Aβ peptides and contribute to AD pathogenesis. To address this issue, we evaluated the role of this receptor in the regulation of APP levels/processing and its influence on cell viability using well-characterized mouse L cells deficient in the expression of the murine IGF-II receptor (MS cells) and corresponding MS9II cells that overexpress the human IGF-II receptor (26, 27). These cell lines have been used extensively to characterize the role of the IGF-II receptor in cell signaling as well as trafficking of lysosomal enzymes (28–30). Using a variety of approaches, we show that the overexpression of the IGF-II receptor enhances APP levels and its processing, leading to the increased production of Aβ peptides. Additionally, our results reveal that an increase in levels of Aβ-related peptides can render MS9II cells more vulnerable to staurosporine-induced toxicity, suggesting a role for the IGF-II receptor in cell viability.

MATERIALS AND METHODS

Materials. NuPAGE 4 to 12% Bis-Tris gels, Alexa Fluor 350/488/594-conjugated secondary antibodies, ProLong Gold antifade reagent, enzyme-linked immunosorbent assay (ELISA) kits for detecting mouse $A\beta_{1-40}$ and $A\beta_{1-42}$, Lipofectamine RNAiMAX transfection reagent, annexin V-Alexa Fluor 594 conjugate, and cholera toxin subunit B (CTXB), which binds to the ganglioside GM1, were purchased from Life Technologies, Corp. (Burlington, ON, Canada). Human IGF-II receptor small interfering RNA (siRNA) and control siRNA were obtained from Dharmacon (Ottawa, ON, Canada). The bicinchoninic acid protein assay kit and enhanced chemiluminescence kit were from ThermoFisher Scientific Inc. (Nepean, ON, Canada). Vivaspin filtration columns were from GE Healthcare Ltd. (Mississauga, ON, Canada). Pitstop2, the Pitstop2 negative control, and the β-secretase enzyme activity assay kit were from Abcam (Cambridge, MA). Staurosporine, γ-secretase inhibitor L-658,458, and OptiPrep were obtained from Sigma-Aldrich (Oakville, ON, Canada). β-Secretase inhibitor IV (BIV) was from Calbiochem (Etobicoke, ON, Canada), and Leu^{27}IGF-II was from GroPep (Adelaide, Australia). Sources of primary antibodies used in the study are listed in Table 1. All horseradish peroxidase-conjugated secondary antibodies were purchased from Santa Cruz Biotechnology (Paso Robles, CA). All other chemicals were from Sigma-Aldrich or ThermoFisher Scientific.

Cell culture. IGF-II receptor-deficient mouse fibroblasts (MS) and corresponding MS cells stably transfected with human IGF-II receptor cDNA, known as MS9II cells, and the human IGF-II receptor cDNA were gifts from W. S. Sly (Saint Louis University, St. Louis, MO) (26, 27, 31). The cells were maintained in Dulbecco's modified Eagle medium (DMEM) supplemented with 0.1 g/liter sodium pyruvate, 2.2 g/liter sodium bicarbonate, 25 U penicillin-streptomycin, 3.2 mM methotrexate, and 5% dialyzed fetal bovine serum. All experiments were performed with MS and MS9II cells between passages 5 and 14. Cells were seeded at 1×10^4 cells/cm^2, and the medium was replaced every 3 to 4 days as described earlier (29). Cultured MS and MS9II cells were harvested at 90% confluence per the requirement of the specific protocol or stored at −80°C until further processing. In some experiments, cells were treated with the IGF-II analogue Leu^{27}IGF-II (10^{-8} and 10^{-7} M) for 20 min or 1 h. To block clathrin-mediated endocytosis, cells were incubated with the endocytosis inhibitor Pitstop2 (10 μM) or the Pitstop2 negative control (32) for 15 and 30 min. The human neuroblastoma cell line SK-N-AS (CRL 2137) was obtained from the American Type Culture Collection (Manassas, VA). These cells were maintained in DMEM plus 10% fetal bovine serum.

Western blotting. Western blotting of cultured cell lysates was performed as described earlier (33). In brief, cells were homogenized with radioimmunoprecipitation lysis buffer containing protease inhibitor cocktail, and proteins were quantified using a bicinchoninic acid assay kit. Denatured samples were resolved on 7 to 17% gradient sodium polyacrylamide or NuPAGE 4 to 12% Bis-Tris gels, transferred to polyvinylidene membranes, blocked with 5% milk, and incubated overnight at 4°C with various primary antibodies at the dilutions listed in Table 1. The following day, membranes were incubated with horseradish peroxidase-conjugated

secondary antibodies (1:5,000), and immunoreactive proteins were detected with enhanced chemiluminescence. All blots were reprobed with anti-β-actin antibody and quantified using an MCID image analysis system (Imaging Research, Inc., St. Catharines, ON, Canada). Western blots for the IGF-II receptor and green fluorescent protein (GFP) were resolved on 8% or 12% SDS-PAGE gels under nondenaturing conditions, transferred to Protran nitrocellulose BA85 membranes, blocked with 4% milk in HEPES-buffered saline, pH 7.6, 0.1% Tween 20, and incubated overnight at 4°C with primary antibodies. Membranes were washed and incubated with secondary goat anti-mouse horseradish peroxidase-conjugated antibodies and detected with enhanced chemiluminescence (34). Signal intensities were quantified using an Amersham Typhoon FLA 7000 imager (GE Healthcare, Pittsburgh, PA).

Immunocytochemistry. For intracellular localization of IGF-II receptors, we performed double immunofluorescence labeling on MS and MS9II cells. In brief, seeded cells (1×10^4 cells/cm^2) on coverslips were fixed with 4% paraformaldehyde (PFA), washed with phosphate-buffered saline (PBS), and then incubated overnight at 4°C with a combination of anti-IGF-II receptor, anti-APP, anti-β-site APP-cleaving enzyme 1 (anti-BACE1), and anti-presenilin 1 (anti-PS1) with or without an organelle marker, such as anticalnexin, anti-Rab5, anti-Rab7, anti-Rab11, and anti-lysosome-associated membrane protein 1 (anti-LAMP1) antibodies at dilutions listed in Table 1. The slides then were exposed to Alexa Fluor 350/488/594-conjugated secondary antibodies (1:1,000) for 2 h, washed, and mounted with ProLong Gold antifade medium. Immunostained cells were visualized using a Zeiss Axioskop-2 fluorescence microscope or a Zeiss LSM 510 confocal microscope, and the images were analyzed with a ZEN 2010 (Carl Zeiss, Germany). The tubular localization of APP was evaluated in 895 MS and 850 MS9II cells from three separate cultures using a Zeiss Axioskop-2 microscope.

β- and γ-secretase activity assays. Cultured fibroblasts were homogenized with radioimmunoprecipitation buffer, centrifuged at 10,000 × *g* for 5 min, and then processed to measure β-secretase activity using the activity assay kit according to the manufacturer's instructions. The fluorescence was measured at an excitation wavelength of 355 nm and emission wavelength of 495 nm. Specific activity was determined by incubating parallel samples with a β-secretase inhibitor provided with the kit. The γ-secretase activity assay was performed on crude membrane fractions as described previously (35), with minor changes. Cultured cells were homogenized in 10 mM Tris-HCl (pH 7.4) containing 1 mM EDTA with protease inhibitor cocktail and then centrifuged to remove nuclei and cell debris. The supernatant was further centrifuged at 100,000 × *g* for 1 h to separate the membrane fraction, which was solubilized in the homogenization buffer, and 25 μg protein was used to measure the γ-secretase activity in 50 mM Tris-HCl (pH 6.8), 2 mM EDTA, and 0.25% CHAPSO {3-[(3-cholamidopropyl)-dimethylammonio]-2-hydroxy-1-propanesulfonic acid} with 8 μM fluorogenic γ-secretase substrate in a 200-μl reaction volume. The fluorescence was measured at an excitation wavelength of 355 nm and emission wavelength of 440 nm, and the specific activity was determined by incubating parallel samples with 100 μM γ-secretase inhibitor L-658,458. All samples were assayed in duplicate, and the data were obtained from four independent experiments.

ELISA for mouse $A\beta_{1-40}$/$A\beta_{1-42}$. Cellular Aβ from cultured cells was solubilized in 5 M guanidine-HCl–50 mM Tris-HCl (pH 8.0) buffer for 4 h, centrifuged at 16,000 × *g* for 20 min, and then assayed for mouse $A\beta_{1-40}$ or $A\beta_{1-42}$ using commercial ELISA kits. For secreted Aβ, conditioned media from cultured cells were concentrated by using Vivaspin-6 filtration columns with a 3,000-molecular-weight cutoff and then analyzed for mouse $A\beta_{1-40}$ or $A\beta_{1-42}$ levels using the ELISA kits. Standard curves generated using synthetic peptides were used to convert signal intensities to picograms per milliliter of mouse $A\beta_{1-40}$ or $A\beta_{1-42}$. All samples were assayed in duplicate, and results presented were obtained from four independent experiments.

IGF-II receptor knockdown by RNA interference. To substantiate the role of IGF-II receptor overexpression on APP levels and metabolism, we transfected MS9II cells with different concentrations of human IGF-II receptor siRNA (10 to 200 nM) or scrambled siRNA (200 nM) using Lipofectamine RNAiMAX transfection reagent. IGF-II receptor knockdown was analyzed 48 h following transfection using Western blotting. These cells subsequently were processed to determine the levels of APP and Aβ-related peptides.

Adenoviral infection. The adenoviral construct containing the wild-type IGF-II receptor cDNA was produced using the AdEasy adenoviral vector system (Agilent Technologies, Santa Clara, CA) by following the manufacturer's instructions. Briefly, the cDNA encoding the full-length, wild-type IGF-II receptor followed by a Myc tag (36) was excised from pBK-cytomegalovirus (CMV) using XhoI and XbaI and cloned into the pShuttle-CMV vector. The shuttle vector was linearized with PmeI and cotransformed into BJ5183 cells with the pAdEasy-1 vector. Recombinant transformants were selected and produced in recombination-deficient DH5α cells. The adenoviral DNA was digested with PacI and transfected into HEK293 cells to produce and package the viral particles. The infectious virus titer using the 50% tissue culture infective dose ($TCID_{50}$) was determined to calculate the multiplicity of infection (MOI). The AdEasy viral construct bearing *Aequorea victoria* GFP was a gift of Tsuneya Ikezu (currently at University of Tokyo, Japan). For the adenoviral transduction expression studies, human neuroblastoma SK-N-AS cells were seeded into dishes in full-growth medium containing 10% serum supplemented with 0.1 mM nonessential amino acids and cultured overnight. Cells were mock infected or transduced with adenovirus containing the wild-type IGF-II receptor or GFP at a multiplicity of infection of 100 in full-growth medium for 3 h, and then the medium was replaced with fresh, virus-free full-growth medium and allowed to acclimate for 48 h. The medium was replaced with reduced-serum Opti-MEM (Life Technologies, Grand Island, NY), and conditioned medium was collected at 24- and 48-h time points following the medium switch. Cells were harvested at 90% confluence at the 48-h time point to prepare lysates.

Isolation of lipid raft and immunoblotting. MS and MS9II cells were lysed on ice in TNE buffer (50 mM Tris-HCl, 150 mM NaCl, 5 mM EDTA, pH 7.4) containing protease inhibitors by passing them through a 20-gauge needle for 10 pulses and a 25-gauge needle for 15 pulses. Cell lysates then were incubated with 1% Triton X-100 in TNE buffer for 30 min at 4°C. Samples were centrifuged at 10,000 × *g* for 5 min at 4°C, and supernatant (250 μl) was adjusted to 40% (wt/vol) OptiPrep with 60% OptiPrep and then overlaid with a 5 to 30% discontinuous OptiPrep gradient on top. Typically, 0.5 ml of 5% OptiPrep and 3 ml of 30% OptiPrep were layered over 1.5 ml of 40% of OptiPrep in a 14-ml tube and then centrifuged at 100,000 × *g* for 24 h at 4°C. The gradients were fractionated into 400-μl aliquots each from the top of the tube and then processed for immunoblotting. Identification of the lipid raft fractions was carried out using anti-caveolin 1 or horseradish peroxidase-conjugated CTXB, which binds to GM1 specifically. For immunoblotting, MS and MS9II lipid raft fractions were subjected to Western blotting with anti-IGF-II receptor, anti-APP (22C11 and Y188), anti-α-disintegrin and metalloprotease 10 (anti-ADAM10), anti-BACE1, anti-PS1, and anti-anterior pharynx defective-1 (anti-APH-1) antibodies at dilutions listed in Table 1. Membranes then were incubated with appropriate horseradish peroxidase-conjugated secondary antibodies (1:5,000) and visualized with enhanced chemiluminescence. All blots were quantified using an MCID image analysis system as described earlier (37).

CTXB surface binding and uptake. MS and MS9II cells grown on coverslips were incubated for 15 min on ice with 4 μg/ml Alexa Fluor 647-conjugated CTXB subunit (AF647-CTXB; Invitrogen) diluted in Hanks' balanced salt solution (HBSS) containing 10 mM HEPES, 3 mM $CaCl_2$, 1.5 mM $MgCl_2$, and 20 mg/ml bovine serum albumin, pH 7.3. For CTXB uptake, cells were warmed in the culture medium for 30 min at 37°C. After washes with HBSS-HEPES buffer, cells were fixed with 4% PFA for 20 min, quenched with 50 mM NH_4Cl for 10 min, and permeabilized with PBS–0.2% Triton X-100 for 5 min at room temperature. Cells were stained for 30 min at room temperature with Hoechst 0.25 μg/ml in

PBS and 0.1 μg/ml phalloidin-tetramethyl rhodamine isocyanate (phalloidin-TRITC) (Sigma) diluted in PBS. Coverslips were mounted with Permafluor, and confocal images were acquired using a Leica SP5 II STED-CW superresolution laser scanning microscope using a 40× (numeric aperture, 1.25) oil objective. All images of CTXB labeling and uptake were acquired using identical settings, and the contrast of all images was adjusted similarly.

Flow cytometry quantification of surface CTXB binding. MS or MS9II cells were trypsinized, and aliquots of 10^6 cells were incubated on ice for 30 min in 250 μl HEPES buffer containing 20 μg/ml AF647-CTXB and 20 mg/ml bovine serum albumin. Between each step, cells were washed by centrifugation for 5 min at 800 rpm and resuspended in ice-cold PBS. Cells were fixed with 3% PFA in PBS for 20 min, washed, and incubated at room temperature for 30 min with 0.5 μg/ml Hoechst diluted in PBS to label nuclei. Surface-bound AF647-CTXB and Hoechst fluorescence intensities were acquired from 10,000 cells using a FACSCanto system (Becton Dickinson) and analyzed using FlowJo software.

Cell viability. MS and MS9II cells were left untreated or were treated with staurosporine (0.01 to 0.25 μM) for 24 h. In some experiments, MS and MS9II cells were cotreated with BIV (0.125, 0.25, and 0.5 μM) along with staurosporine (0.1 μM) for 24 h. The cells then were processed to measure cell viability using the 3-(4,5-dimethylthiazol-2-yl)-2,5-diphenyltetrazolium bromide (MTT) assay and annexin V staining. In brief, cells for MTT assay were incubated for 4 h with MTT (0.5 mg/ml in 0.01 M PBS) at 37°C with 5% CO_2–95% air. The formazan was dissolved in dimethyl sulfoxide, and absorbance was measured at 570 nm with a microplate reader. As for annexin V staining, control and treated cells were stained with annexin V-Alexa Fluor 594 conjugate in 10 mM HEPES, 140 mM NaCl, and 2.5 mM $CaCl_2$, pH 7.4, for 15 min at 37°C according to the manufacturer's instructions. Cells were washed with PBS, fixed with 4% PFA, stained with 4′,6-diamidino-2-phenylindole (DAPI), and then visualized using a Zeiss Axioskop-2 fluorescence microscope. Photomicrographs of stained cells were analyzed using ImageJ to calculate the ratios of annexin V-positive and -negative cells in different treatment groups.

Statistical analysis. All results were expressed as means ± standard errors of the means (SEM). Comparisons between different groups were performed using Student's *t* test (two groups) or one-way and two-way analysis of variance (ANOVA) (three or more groups), followed by Bonferroni's *post hoc* analysis, with significance set at $P < 0.05$.

RESULTS

IGF-II receptor overexpression increases levels of APP and its processing to Aβ. Using Western blotting and immunocytochemistry, we validated that MS cells did not express detectable levels of IGF-II receptor, while the receptor is overexpressed in MS9II cells (Fig. 1A and B). To determine the influence of receptor overexpression on APP levels and metabolism, we evaluated protein levels of APP and its secretases in MS and MS9II cells by immunoblot analysis. We found that the levels of APP holoprotein were increased in MS9II cells; this observation is consistent with our previous study, where we reported an increase in APP transcript levels (38). However, the levels of the APP homolog APLP1 were decreased in MS9II compared to MS cells, suggesting a rather selective effect of the IGF-II receptor on increased APP levels (Fig. 1C and D).

As for APP secretases, our immunoblot results revealed that α-secretase ADAM10 levels remained unaltered (Fig. 1E), and BACE1 levels were increased (Fig. 1F) in MS9II cells compared to the levels in MS cells. In a previous study, we found that two subunits of γ-secretase complex (PS1 and APH1) were unaffected by IGF-II receptor overexpression (38). Analysis of APP cleavage products showed that the levels of APP–CTF-α and APP–CTF-β, generated by α- and β-secretases, respectively, were markedly increased in MS9II cells compared to the levels in MS cells (Fig. 1G), but the ratio of APP-CTFs to full-length APP levels was not different between the two cells (data not shown). The increase in CTF levels was accompanied by elevated levels of soluble APP fragments (sAPPα and sAPPβ) in the conditioned media of MS9II cells (Fig. 1H). The levels of total murine $Aβ_{1–40}$ and $Aβ_{1–42}$, as detected by ELISA, also were significantly increased in the conditioned media but not in the cell lysates of MS9II cells (Fig. 2A and B). In addition to the levels of APP derivatives, we also measured the activities of APP secretases in these cells. Interestingly, both β- and γ-secretase enzyme activities were higher in MS9II cells than in MS cells (Fig. 2C and D). Finally, to assess whether differences in enzymatic degradation of Aβ could contribute to the observed differences in Aβ levels, we measured the steady-state levels of neprilysin and insulin-degrading enzyme (IDE) in both cell lines by immunoblotting. Our results clearly showed that levels of IDE but not neprilysin were significantly lower in MS9II cells than in MS cells (Fig. 2E and F). Thus, IGF-II receptor overexpression increases $Aβ_{1–40}/Aβ_{1–42}$ levels by increasing the levels and enhancing the processing of APP and possibly by reducing Aβ degradation. Evidence suggests that the activation of certain cell surface receptors can alter the levels and/or processing of APP (5, 6). Although stimulation of the IGF-II receptor in MS9II cells with Leu^{27}IGF-II enhanced intracellular phosphoprotein kinase Cα (PKCα) levels as expected (39), it did not significantly alter the levels of APP or its cleaved products, APP–CTF-α/APP–CTF-β (data not shown). Additionally, the levels of full-length APP and APP-CTFs remained unaltered following transient blockade of clathrin-mediated endocytosis by Pitstop2 in MS9II cells (data not shown).

Significance of IGF-II receptor in regulating APP level/metabolism. To validate the requirement for continued overexpression of the IGF-II receptor for the observed increase in APP expression and metabolism, we knocked down receptor expression in MS9II cells using human IGF-II receptor-specific siRNA and evaluated levels of APP and its cleaved products, as well as BACE1. As expected, IGF-II receptor-targeting siRNA dose dependently (10 to 200 nM) decreased receptor levels 48 h after transfection compared to those with scrambled siRNA (Fig. 3A and B). Interestingly, the decrease in IGF-II receptor in MS9II cells is accompanied by a concomitant decrease in the levels of APP holoprotein, BACE1, and APP-CTFs (Fig. 3B to G). Furthermore, the levels of $Aβ_{1–40}$ and $Aβ_{1–42}$, as measured by ELISA, also were significantly reduced in the conditioned media of MS9II cells transfected with human IGF-II receptor siRNA (Fig. 3H). Together, these results suggest that continued overexpression of the IGF-II receptor is indeed involved in the upregulation of APP and its metabolism, leading to the increased production of Aβ peptides.

Localization of the IGF-II receptor, APP, and its processing enzymes. Earlier studies have shown that APP and its processing enzymes localize to several secretory and endocytic organelles (5, 6, 21, 22). To determine whether the overexpression of the IGF-II receptor can alter its subcellular distribution, we used immunofluorescence labeling to assess the localization of APP, BACE1 (Fig. 4 and 5), and PS1 (data not shown), along with markers of the endoplasmic reticulum (ER), early endosomes, late endosomes, and lysosomes. First, we observed that a subset of APP, BACE1 (Fig. 4 and 5A to D), and PS1 (data not shown) in the perinuclear region colocalized with the IGF-II receptor in MS9II

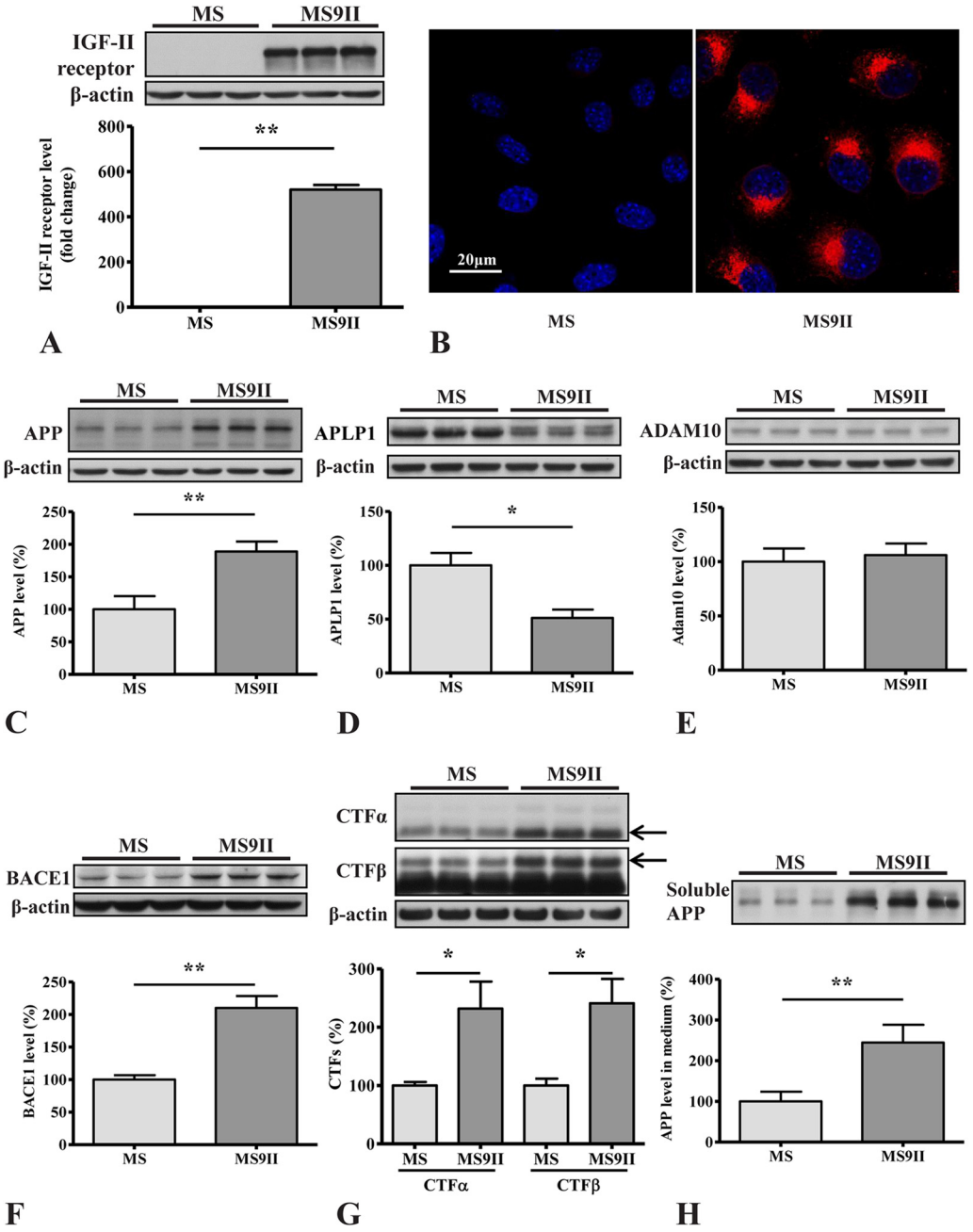

FIG 1 (A and B) Western blotting (A) and immunofluorescence staining (B) validating increased levels and expression of IGF-II receptor in MS9II versus MS cells. (C to E) Immunoblots and respective histograms showing increased levels of APP holoprotein (C), decreased levels of homologous APLP1 protein (D), and unaltered levels of ADAM10 (E) in IGF-II receptor-overexpressing MS9II cells. (F to H) Immunoblots and respective histograms showing increased levels of BACE1 (F), APP-CTFs (CTF-α and CTF-β) (G), and soluble APP fragments (sAPPα and sAPPβ) (H) in MS9II cells versus MS cells. All Western blots were reprobed with β-actin antibody to monitor protein loading, and the values, expressed as means ± SEM, were from 3 or 4 independent experiments. Data were analyzed using Student's *t* test. *, $P < 0.05$; **, $P < 0.01$. Scale bar, 20 μm.

cells. Second, as expected from the increased steady-state levels observed by immunoblot analysis, MS9II cells had relatively higher levels of APP and BACE1 immunofluorescence than MS cells (Fig. 4 and 5A to D). Intriguingly, APP immunoreactivity in MS9II cells but not in MS cells was apparent in discrete tubular structures emanating from the perinuclear region. On the other hand, APP in MS cells was highly concentrated in cellular protrusions (Fig. 4). Aside from this striking redistribution of APP, we did not observe specific differences in the colocalization of APP with the organelle markers, such as calnexin (ER), Rab5 (early endosomes), Rab7 (late endosomes), Rab11 (recycling endosomes), or LAMP1 (lysosomes), when analyzed by confocal microscopy (Fig. 4E to X). In MS9II cells, BACE1 was localized mainly to intracellular vesicles that were positive for endosomal markers (Rab5 and Rab7) and, to a lesser extent, in LAMP1-labeled lysosomes and calnexin-labeled ER. In the ab-

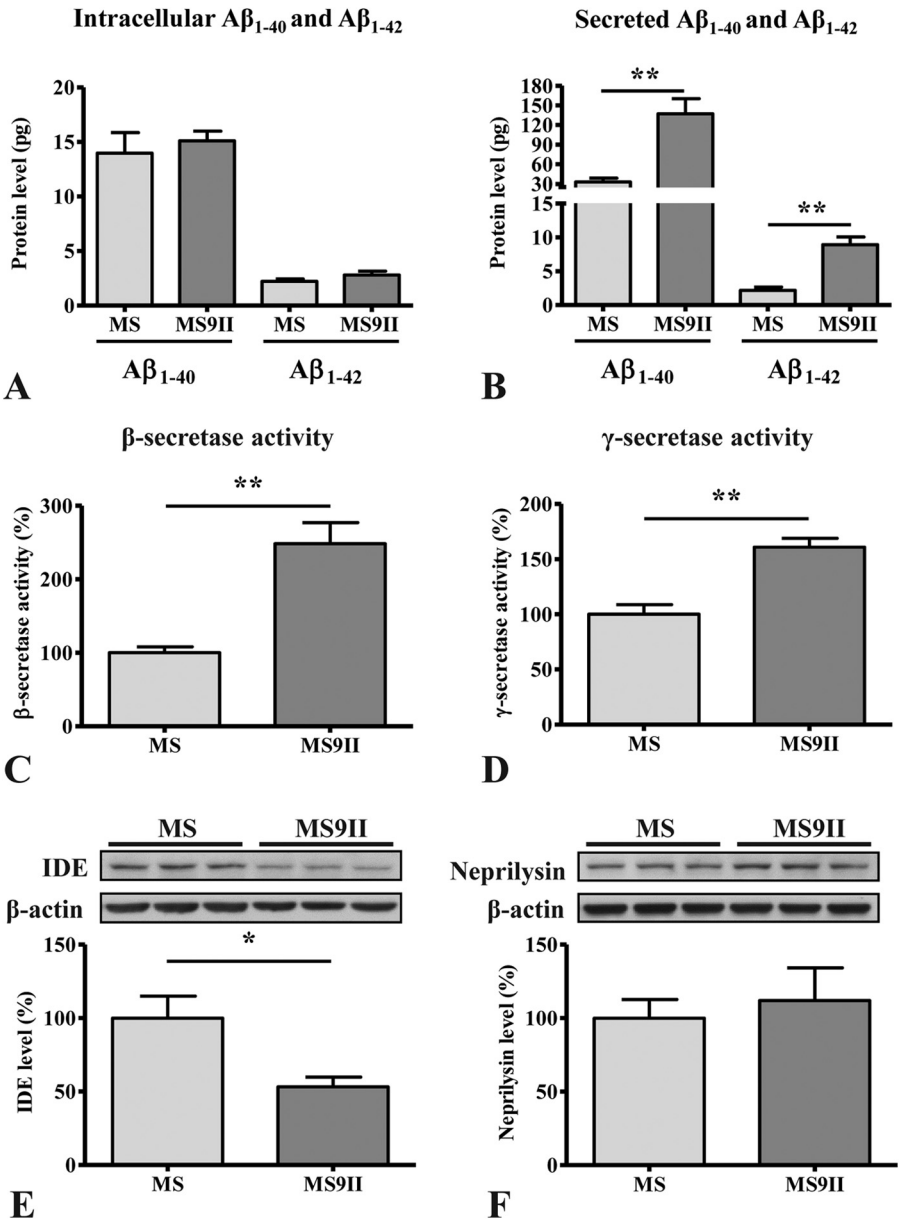

FIG 2 (A and B) Histograms showing $A\beta_{1-40}$ and $A\beta_{1-42}$ levels in the cell lysates (A) and conditioned media (B) of MS9II and MS cells as detected by ELISA. Note the increased levels of $A\beta_{1-40}$ and $A\beta_{1-42}$ in the media but not in the cell lysates of MS9II cells compared to that in MS cells. (C and D) Histograms depicting increased activity of β-secretase (C) and γ-secretase (D) complex in MS9II cells compared to that in MS cells. (E and F) Immunoblots and respective histograms showing decreased levels of insulin-degrading enzyme (IDE) (E) and unaltered levels of neprilysin (F) in IGF-II receptor-overexpressing MS9II cells compared to those in MS cells. All Western blots were reprobed with β-actin antibody to monitor protein loading, and the values, expressed as means ± SEM, were from 3 or 4 independent experiments. Data were analyzed using Student's *t* test. *, $P < 0.05$; **, $P < 0.01$.

sence of IGF-II receptor expression, BACE1 immunoreactivity still appeared to be higher in early and late endosomes than in other organelles but also was present in cellular protrusions (Fig. 5E to T). PS1 localization in intracellular organelles did not appear to differ appreciably between MS and MS9II cells (data not shown). These results, taken together, suggest that IGF-II receptor overexpression not only enhanced the levels of APP and BACE1 but also, to some extent, influenced their distributions within the cells.

Association of the IGF-II receptor, APP, and its processing enzymes with lipid rafts. Evidence suggests that the α-secretase ADAM10 resides mostly in the low-cholesterol-containing nonraft domains (40), whereas a subset of BACE1 and γ-secretase complex is associated with cholesterol-rich lipid raft microdomains of the plasma membrane and intracellular organelles (41, 42). APP, on the other hand, exists in both the raft and nonraft microdomains of the cellular membranes (43, 44). These observations raised the possibility that amyloidogenic versus nonamyloidogenic processing of APP occurs in different microdomains of the membrane, but an alteration in the distribution of APP or its processing enzymes influences APP processing. To determine whether the overexpression of the IGF-II receptor can enhance

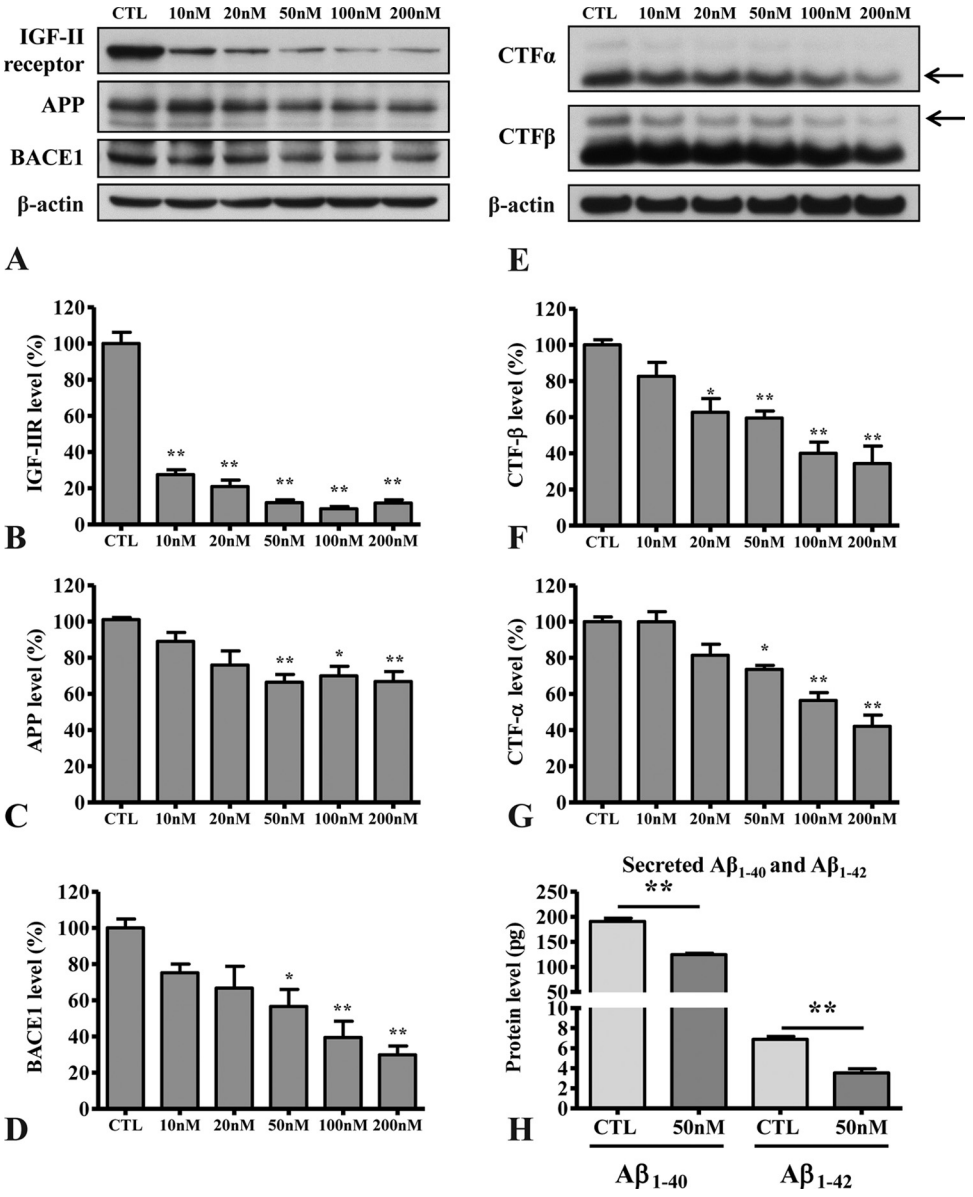

FIG 3 (A to D) Immunoblots (A) and respective histograms showing levels of IGF-II receptor (B), APP holoprotein (C), and BACE1 (D) in MS9II cells following 48-h treatments with control scramble siRNA at 200 nM and human IGF-II receptor siRNA at 10, 20, 50, 100, and 200 nM. CTL, control. (E to G) Immunoblots (E) and respective histograms showing levels of APP–CTF-α (F) and APP–CTF-β (G) in MS9II cells following 48-h treatments with control scramble siRNA at 200 nM and human IGF-II receptor siRNA at 10, 20, 50, 100, and 200 nM. Note the dose-dependent effects of human IGF-II receptor siRNA in decreasing not only the levels of the receptor but also the levels of APP, BACE1, and APP-cleaved products. (H) Histogram showing decreased levels of secretory $A\beta_{1-40}$ and $A\beta_{1-42}$ in the conditioned media of MS9II cells following 48 h of treatment with 50 nM human IGF-II receptor siRNA compared to that with 50 nM control scramble siRNA. All Western blots were reprobed with β-actin antibody to monitor protein loading, and the values, expressed as means ± SEM, were from 3 independent experiments. Data of Aβ secretion were analyzed using Student's *t* test, whereas dose-dependent effects of siRNA treatment were analyzed using one-way ANOVA followed by Bonferroni's *post hoc* analysis. *, $P < 0.05$; **, $P < 0.01$.

amyloidogenic processing of APP by influencing membrane microdomain redistribution of APP or its processing enzymes, we analyzed MS and MS9II cells by lipid raft fractionation. Cells were lysed with 1% Triton X-100 on ice, followed by discontinuous OptiPrep gradient centrifugation to separate the detergent-resistant microdomains from the detergent-soluble nonraft domains. The presence of major constituents of lipid rafts, namely, GM1 and caveolin 1 in fractions 3 to 5, and the nonraft marker transferrin receptor in fractions 8 to 12 validated our fractionation protocol (Fig. 6A). Whereas the majority of the IGF-II receptor was found in nonraft fractions, a small fraction was found in the raft fractions (Fig. 6A and B). Consistent with published studies (44), APP and its metabolites, BACE1 and PS1, were found in Triton X-100-resistant raft fractions in MS9II and MS cells (Fig. 6A). Overall, the relative amounts of BACE1, PS1, and APP-CTFs (APP–CTF-α and APP–CTF-β) found in lipid raft versus nonraft fractions were similar between MS9II and MS cells (data not shown). However, the relative proportion of full-length APP mol-

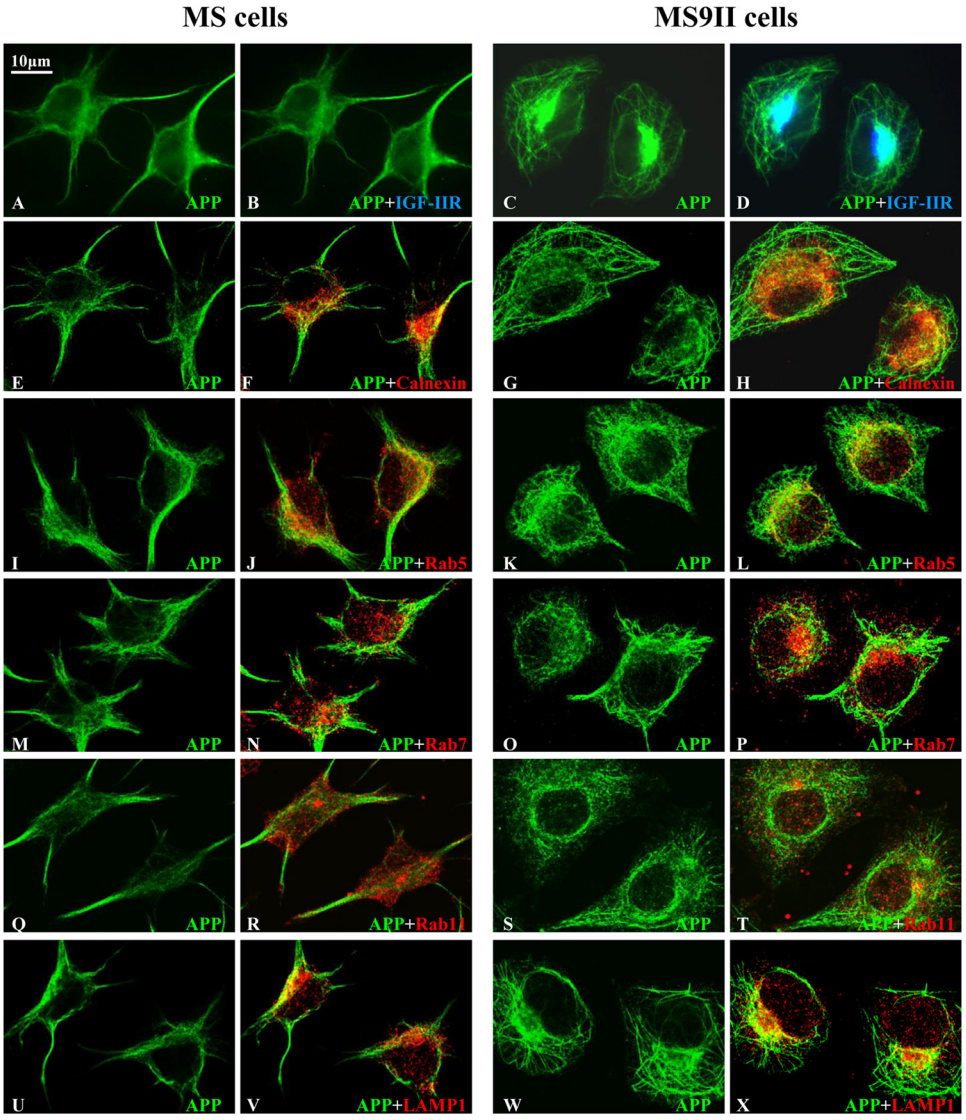

FIG 4 (A to D) Representative immunofluorescence images of MS and MS9II cells showing localization of APP with the IGF-II receptor. Note the localization of a subset of APP with IGF-II receptor in MS9II cells. (E to T) Confocal images of MS and MS9II cells depicting localization of APP (E, G, I, K, M, O, Q, and S) in calnexin-labeled ER (F and H), Rab5-labeled early endosomes (J and L), Rab7-labeled late endosomes (N and P), Rab11-labeled recycling endosomes (R and T), and LAMP1-labeled lysosomes (V and X). IGF-II receptor, as expected, was not detected in MS cells. APP immunoreactivity was more evenly distributed in the ER, endosomes, and lysosomes in MS cells than in MS9II cells.

ecules recovered in the raft fractions was significantly higher in MS9II cells than in MS cells (Fig. 6C).

In our fractionation experiments, we noticed that the levels of the glycosphingolipid GM1 and the caveolar coat protein caveolin 1, but not the levels of transferrin receptor, were significantly higher in MS9II than in MS cells (Fig. 6A). We confirmed these observations using quantitative immunoblot analysis of whole-cell lysates (data not shown). Lipid rafts are heterogeneous and dynamic membrane microdomains enriched in sphingolipid and cholesterol. Previous studies revealed that CTXB bound to cell surface GM1 is internalized by clathrin-dependent as well as by dynamin-independent raft endocytic pathways (45). Interestingly, overexpression of caveolin 1 is known to attenuate internalization of CTXB to the Golgi apparatus (46). Since MS9II cells have higher levels of GM1 and caveolin 1, we performed CTXB surface binding and internalization assays in order to ascertain raft-mediated endocytosis of GM1. First, we incubated MS and MS9II cells on ice with Alexa Fluor 647-labeled CTXB to stain cell surface GM1, followed by Hoechst to stain the nuclei, and analyzed fluorescence intensities by flow cytometry. The results showed that the majority of MS9II cells had significantly higher levels of CTXB binding (Fig. 7A and B). Second, we stained cells grown on coverslips with CTXB on ice to label surface GM1 and fixed them prior to staining with phalloidin and Hoechst to visualize F-actin and nuclei, respectively. One set of coverslips was warmed for up to 30 min at 37°C to allow the internalization of CTXB prior to fixation. In agreement with the flow cytometry results, confocal microscopy analysis revealed that the majority of MS9II cells had markedly high levels of surface CTXB fluorescence (Fig. 7C). The CTXB fluorescence appears to be on the plasma

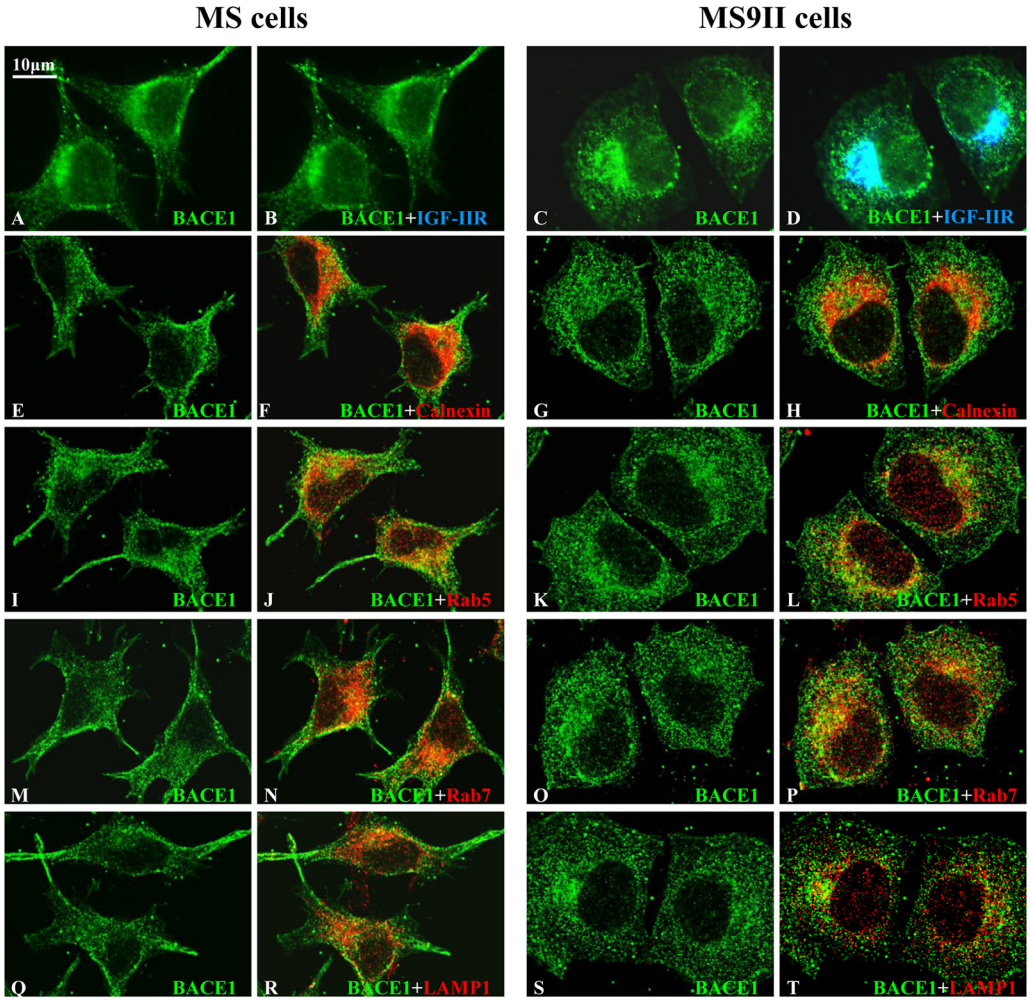

FIG 5 (A to D) Representative immunofluorescence images of MS and MS9II cells showing localization of BACE1 with IGF-II receptor. Note the localization of a subset of BACE1 with IGF-II receptor in MS9II cells. (E to T) Confocal images of MS and MS9II cells depicting localization of BACE1 (E, G, I, K, M, O, Q, and S) in calnexin-labeled ER (F and H), Rab5-labeled early endosomes (J and L), Rab7-labeled late endosomes (N and P), and LAMP1-labeled lysosomes (R and T). IGF-II receptor, as expected, was not detected in MS cells. BACE1 immunoreactivity was more evenly distributed in the ER, endosomes, and lysosomes in MS cells than in MS9II cells.

membrane when the coverslips were fixed immediately after CTXB labeling, whereas it appears predominantly in the perinuclear area after internalization for 30 min (Fig. 7D). These results indicate that MS9II cells have high levels of GM1, and that CTXB internalization is not disrupted in these cells despite higher levels of caveolin 1 expression. Together with raft fractionation results, these findings provide a basis to suggest that IGF-II receptor overexpression influences the processing of APP, leading to enhanced levels of Aβ peptides partly by increasing the levels of lipid raft microdomain components and shifting more full-length APP to membrane raft microdomains.

Enhanced Aβ production increases cell vulnerability to toxicity. Earlier studies have shown that increased levels of APP–CTF-β and Aβ peptides can render cells more susceptible to toxicity (47, 48). To determine whether IGF-II receptor-overexpressing MS9II cells, which generate higher levels of APP–CTF-β and Aβ peptides, are more susceptible to toxicity than MS cells, we exposed both cell lines for 24 h to 0.01 to 0.25 μM staurosporine, a broad-spectrum protein kinase inhibitor that has been used widely to induce apoptosis in a variety of cultured cells (49, 50). Our results revealed that staurosporine induced cytotoxicity in a dose-dependent manner in both cell lines, but MS9II cells were significantly more vulnerable to toxicity than MS cells (Fig. 8A). Importantly, toxicity induced by staurosporine was markedly attenuated when the MS9II cells, but not MS cells, were cotreated with various concentrations of the β-secretase inhibitor BIV (Fig. 8B to D). This is accompanied by a dose-dependent decrease of Aβ secretion from MS9II cells treated with staurosporine and BIV (Fig. 8E). These results indicate that enhanced sensitivity to staurosporine is due to increased levels and processing of APP via the amyloidogenic pathway in MS9II cells.

IGF-II receptor overexpression increases levels of APP and its processing in SK-N-AS neuroblastoma cells. To determine whether the overexpression of IGF-II receptor in a neuronal cell line can influence APP levels and its processing, as observed in MS9II cells, we performed a set of experiments using human SK-N-AS neuroblastoma cells, a cellular model widely used to study APP metabolism and neuronal vulnerability. SK-N-AS cells were mock infected or

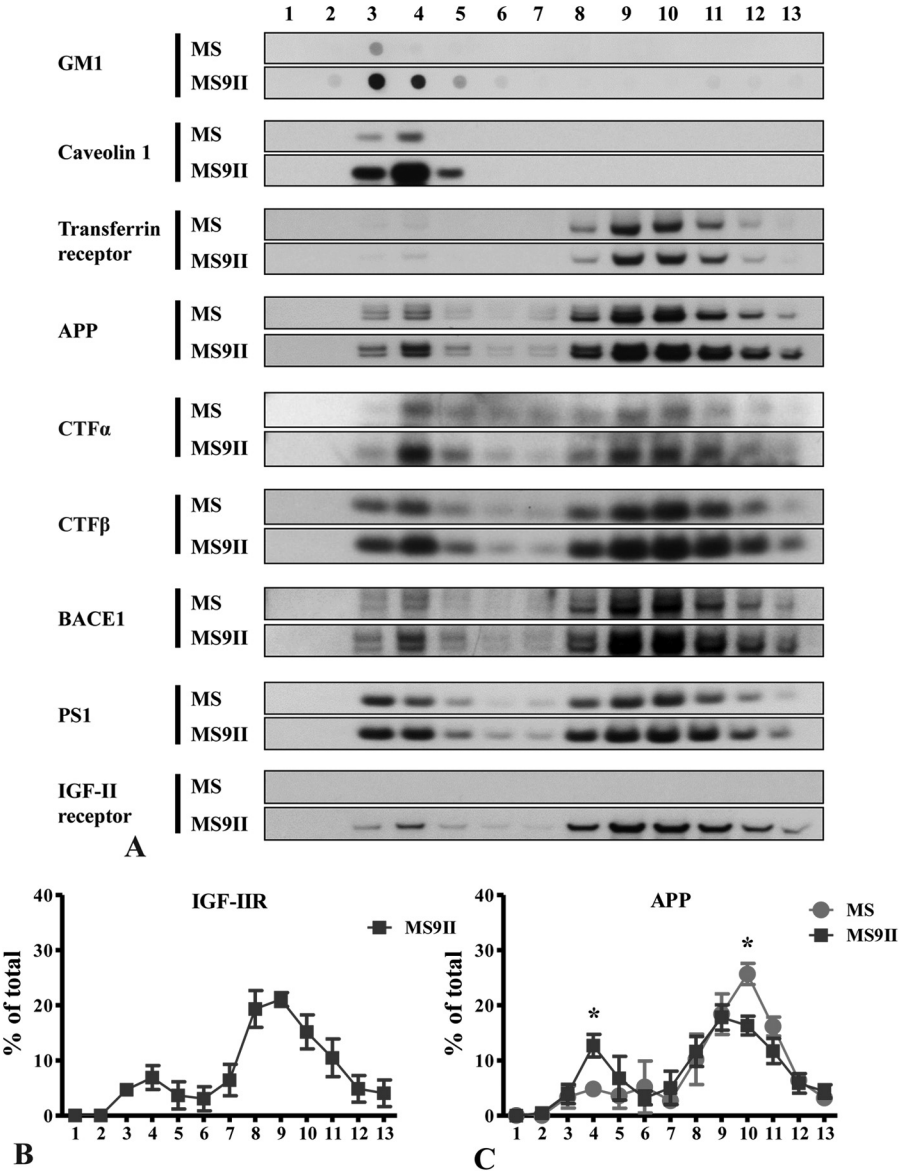

FIG 6 (A) Distribution profiles of IGF-II receptor, APP, BACE1, PS1, and CTFs (CTF-α and CTF-β) on lipid raft and nonraft membrane domains of MS and MS9II cells. Cultured MS and MS9II cells were solubilized in 1% Triton X-100 and fractionated on a discontinuous OptiPrep gradient. Equal volumes of the recovered fractions were separated by SDS-PAGE for the immunoblot analysis using antibodies against the aforementioned proteins. GM1 and caveolin 1 were used as lipid raft markers, whereas transferrin receptor was used as a nonraft marker. Note that IGF-II receptor, APP, BACE1, PS1, CTF-α, and CTF-β are evident both in raft and nonraft domains of the membranes but are found more predominantly in the raft domain in MS9II cells than in MS cells. (B and C) Quantitative analysis of raft distribution of IGF-II receptor and APP. Three independent OptiPrep gradient fractionated samples of MS9II and MS cells were analyzed by immunoblotting and quantified. Data for individual proteins are expressed as percentages of total protein in the blot. Note that the levels of APP were increased in raft fractions but decreased in nonraft fractions of MS9II cells compared to those of MS cells. All values are expressed as means ± SEM, and data were analyzed using Student's *t* test. *, $P < 0.05$.

transduced with adenoviral constructs bearing cDNAs for GFP or the IGF-II receptor. Using Western blot analysis, we first validated that the IGF-II receptor-infected SK-N-AS cells overexpress IGF-II receptor 15-fold relative to endogenous levels of the receptor in cells infected with the GFP vector or mock, uninfected cells (Fig. 9A and B). Our results also revealed that IGF-II receptor overexpression enhanced the levels of APP, APP–CTF-α, and APP–CTF-β in SK-N-AS cells compared to those of cells infected with the GFP vector or uninfected control cells (Fig. 9C to E). Additionally, we observed that levels of secretory $A\beta_{1-42}$ also were increased in the conditioned media of IGF-II receptor-overexpressing cells compared to levels for the controls, but this increase did not reach statistical significance (Fig. 9F). Collectively, these results suggest that the overexpression of the IGF-II receptor can upregulate APP and its metabolism in human SK-N-AS neuroblastoma cells as a representative example of a neuronal cell type.

DISCUSSION

The present study shows that stable IGF-II receptor overexpression in a well-characterized cell culture model increases the levels

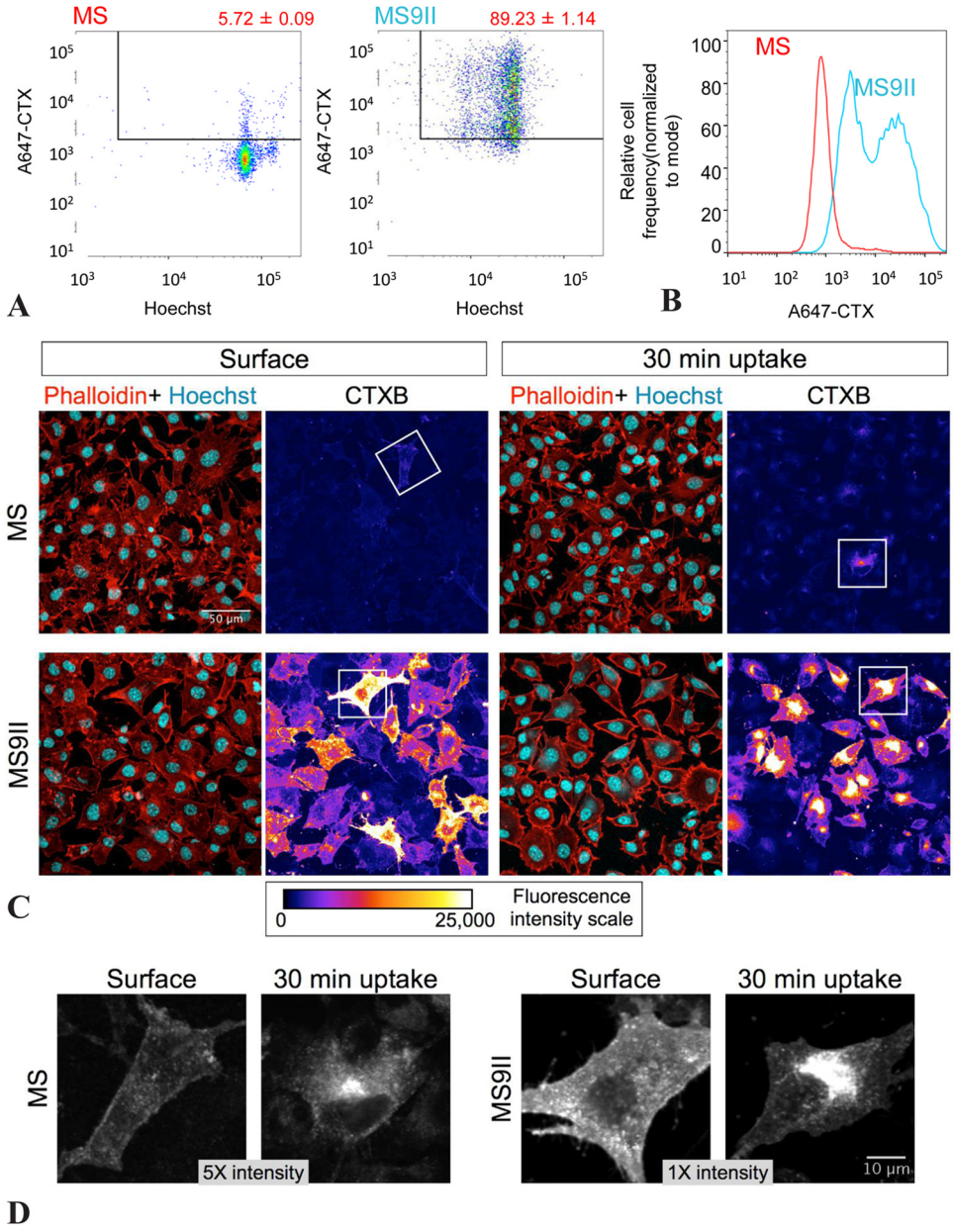

FIG 7 (A) Flow cytometry analysis of surface CTX labeling. Representative dot plots showing AF647-CTX and Hoechst fluorescence in MS versus MS9II cells. (B) The histogram plot shows the frequency distribution of A647-CTX fluorescence intensity of MS (red) and MS9II (blue) cells. (C) MS and MS9II cells were labeled with CTX at 4°C and fixed immediately (Surface) or following 30 min of incubation at 37°C (30 min uptake). The cells were analyzed by confocal microscopy, and AF647-CTX fluorescence intensity of representative MS and MS9II cells is depicted as pseudocolor images. Phalloidin-TRITC and Hoechst overlay images of the same field also are shown. (D) Higher magnification of cells (indicated with boxes in panel C) with brightness and contrast readjusted to visualize the cell surface (Surface) or intracellular localization of CTX (30 min uptake) in MS and MS9II cells. Note that the MS cells are displayed at five times the intensity of the MS9II cells. **, $P < 0.01$.

of $A\beta_{1-40}$ and $A\beta_{1-42}$ by enhancing the levels and processing of endogenous APP. MS9II cells, which overexpress IGF-II receptor, differ from MS cells in four characteristics that contribute to this outcome. First, the levels of APP and BACE1 proteins are increased in MS9II cells. Second, MS9II cells have increased β- and γ-secretase enzyme activities. Third, intracellular localization of APP and BACE1 appears to be somewhat altered in MS9II cells. Fourth, MS9II cells have higher levels of lipid raft components GM1 and caveolin 1 and increased partitioning of full-length APP into rafts, as well as increases in the steady-state localization of APP, BACE1, and PS1 (the catalytic subunit of γ-secretase) in the raft domains. These observations provide a cellular basis for the increased generation of Aβ peptides in MS9II cells. This is supported by our observations in IGF-II receptor-overexpressing SK-N-AS cells, which exhibited increased levels of APP and its cleaved products. Finally, we show that MS9II cells are more vulnerable to staurosporine-induced toxicity, which can be attenuated by a BACE1 inhibitor. Collectively, these results suggest that IGF-II

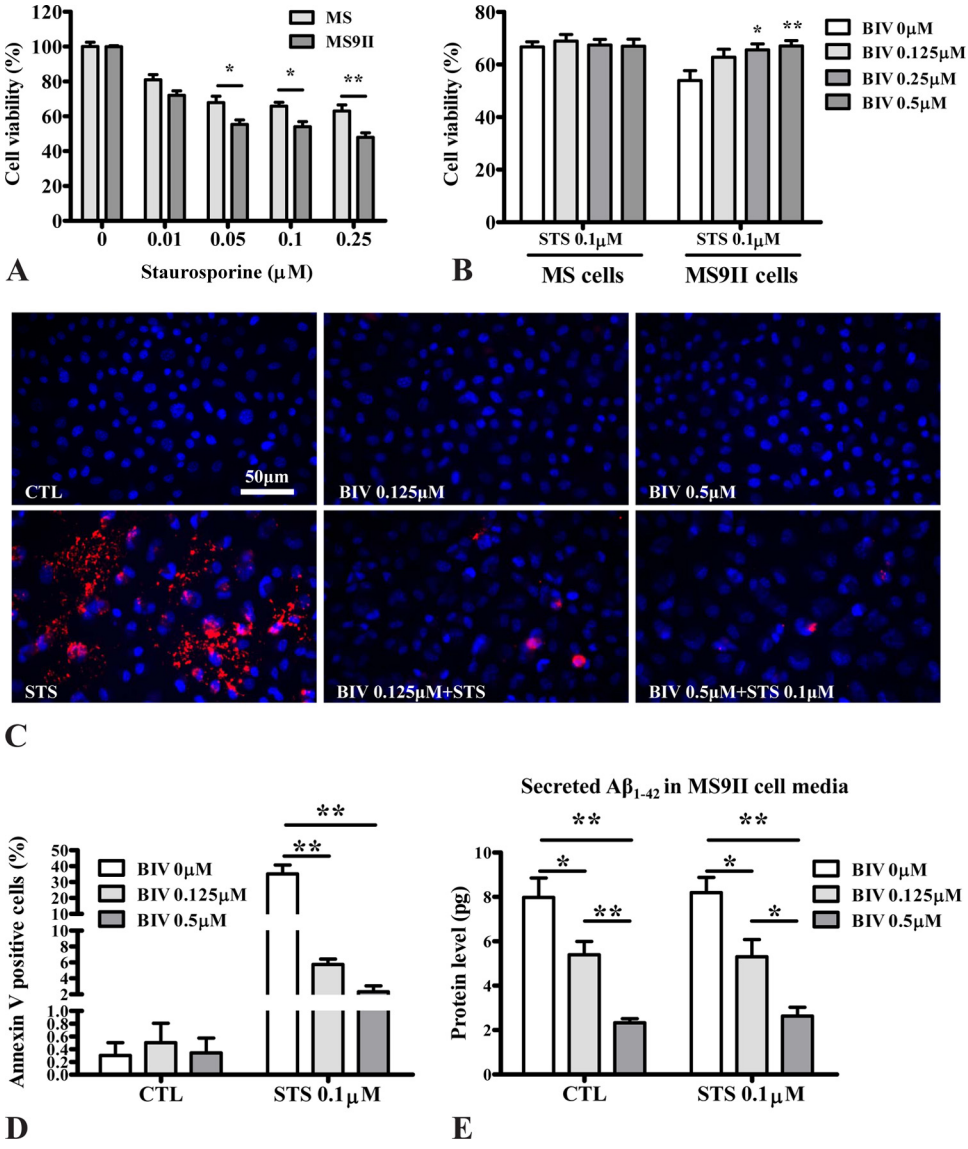

FIG 8 (A) Histogram depicting decreased viability of MS9II versus MS cells following 24 h of treatment with staurosporine (0.01 to 0.25 μM) according to the MTT assay. (B) Histogram showing reduced staurosporine (0.1 μM)-induced toxicity following cotreatment of the cells with different concentrations (0 to 0.5 μM) of β-secretase inhibitor BIV. (C and D) Photomicrographs of annexin V-labeled apoptotic cells (C) and corresponding histogram (D) showing reduced staurosporine (0.1 μM)-induced toxicity following cotreatment of MS9II cells with different concentrations (0.125 and 0.5 μM) of the β-secretase inhibitor BIV. (E) Histogram showing reduced levels of $A\beta_{1-42}$ in the conditioned media of MS9II cells following 24 h of treatment with 0.125 and 0.5 μM BIV and 0.1 μM staurosporine compared to the levels of the untreated control cells. All Western blots were reprobed with β-actin antibody to monitor protein loading. All values are expressed as means ± SEM ($n = 4$), and data were analyzed using two-way ANOVA followed by Bonferroni's *post hoc* analysis. *, $P < 0.05$; **, $P < 0.01$. STS, staurosporine.

receptor overexpression enhances the levels and processing of APP, leading to increased production of Aβ peptides, which may render cells more susceptible to toxicity.

Influence of IGF-II receptor overexpression on APP and its processing enzymes. Previous studies have shown that IGF-II receptor levels usually are not altered in AD brains (23, 24) but are found to be selectively decreased in the hippocampus of AD patients carrying two copies of the *APOE* ε4 allele (23) or is increased in the cortical region of familial cases with a *PSEN1* mutation (24). Notwithstanding the results from AD brains, IGF-II receptor levels are markedly increased in the hippocampus and cortex but not in the striatum of mutant APP transgenic mice compared to those of age-matched controls (25). We recently reported that the overexpression of the IGF-II receptor in MS9II cells increases the steady-state levels of transcripts corresponding to APP, BACE1, and PS1, although the mechanism associated with this transcriptional regulation remains unclear at this point (38). In the present study, we observed that levels of APP and APP-CTFs are increased in MS9II cells as well as in SK-N-AS human neuroblastoma cells overexpressing IGF-II receptor, suggesting a role for the receptor in regulating the levels of APP and its processing. As for secretase, while BACE1 protein levels are increased, the steady-state levels of PS1 as well as those of another γ-secretase subunit, APH-1, are not altered in MS9II cells compared to those in MS cells (34). This

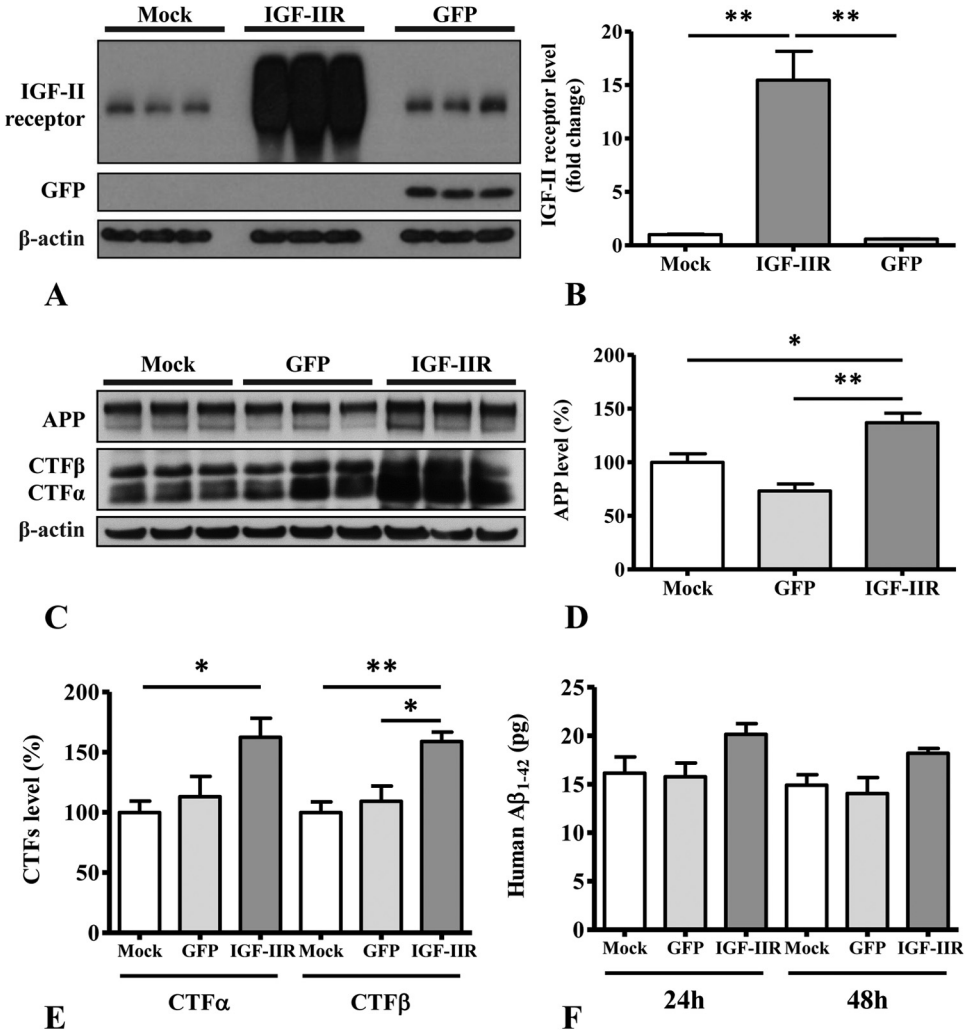

FIG 9 (A and B) Immunoblots (A) and respective histogram (B) showing levels of IGF-II receptor in human SK-N-AS neuroblastoma cells following infection with adenoviral constructs for the IGF-II receptor and green fluorescent protein (GFP) versus mock-infected cells. (C to E) Immunoblots (C) and respective histograms showing increased levels of APP (D) and APP-CTFs (E) in IGF-II receptor overexpressing SK-N-AS neuroblastoma cells compared to levels in mock-infected and uninfected control cells. (F) Histogram showing levels of secretory $A\beta_{1-42}$ in the conditioned media of human SK-N-AS neuroblastoma cells transduced with the IGF-II receptor or GFP compared to that of mock-infected cells at 24 and 48 h after infection. All Western blots were reprobed with β-actin antibody to monitor protein loading, and the values, expressed as means ± SEM, were from 2 or 3 independent experiments. All data were analyzed using Student's *t* test. *, $P < 0.05$; **, $P < 0.01$.

finding is consistent with earlier studies, which showed that steady-state levels of the four γ-secretase complex subunits (PS1/PS2, nicastrin, APH-1, and PEN2) are tightly regulated by their stoichiometric interaction and ability to form stable γ-secretase complex (51–53). At the cellular level, in addition to an overall increase in the levels of APP and BACE1, the overexpression of the IGF-II receptor promoted APP localization in tubular structures, whose exact nature and functional significance remain to be defined. Moreover, MS9II cells showed pronounced perinuclear BACE1 localization compared to that of MS cells. Understanding how these subtle differences in APP and BACE1 localization in MS9II cells contribute to enhanced APP processing would require detailed live-cell imaging studies in the future.

Influence of IGF-II receptor overexpression on the production/clearance of Aβ peptides. The steady-state levels of Aβ are regulated by multiple factors that can influence not only the generation but also the clearance of the peptides (5, 54–56). With regard to APP processing, our results show that IGF-II receptor overexpression can significantly increase APP and APP-CTFs in cell lysates as well as soluble APP in the conditioned media of cultured MS9II cells. These changes are accompanied by an increase of $A\beta_{1-40}$ and $A\beta_{1-42}$ levels in the conditioned media of cultured MS9II cells. The intracellular levels of $A\beta_{1-40}$ and $A\beta_{1-42}$, however, were not markedly different in MS9II cells than in MS cells, suggesting that IGF-II receptor overexpression leads to enhanced production followed by the secretion of Aβ peptides. This is supported by the observed increases in activity of both β- and γ-secretases in MS9II cells. Moreover, a recent quantitative proteomics study revealed that the IGF-II receptor is a BACE1 substrate, and BACE1-mediated IGF-II receptor ectodomain shedding can reduce the number of intact receptors involved in lysosomal transport (57). Since IGF-II receptors mediate intracel-

lular trafficking of lysosomal enzymes, such as cathepsins B and D, which are involved in regulating Aβ metabolism (7–9, 22, 58, 59), it is possible that overexpression of the receptor can influence amyloidogenic processing of APP by altering the levels and/or redistribution of the enzymes within the EL compartments. In this regard, the overexpression of cation-dependent mannose 6-phosphate receptor also has been shown to increase the production of Aβ peptides in cultured mouse fibroblasts by redistribution of lysosomal hydrolases (60). However, it is of interest that neither the activation of the receptor by its agonist Leu^{27}IGF-II nor transient blockade of the clathrin-dependent endocytosis significantly affect the levels or processing of the APP in MS9II cells. Thus, it is likely that the receptor mediates the effects by increasing APP levels and its redistribution within the cells.

Several classes of proteins are known to regulate intracellular sorting of IGF-II receptors. A family of Golgi membrane-localized γ-ear-containing ARF binding (GGA) proteins mediates both the anterograde trafficking of IGF-II receptor from TGN to endosomes as well as retrograde trafficking from endosomes to the TGN (61–63). Retrieval of the IGF-II receptor from endosomes to the TGN is directed by a complex of adaptor proteins, termed retromers, which are composed of two subcomplexes: one, consisting of Vps35p, Vps29p, and Vps26p proteins, involves in cargo selection, and the other is comprised of SNX1/SNX2-SNX5/SNX6 dimers that regulate the formation of membrane tubules. Several other proteins also have been implicated in the retrieval of the IGF-II receptor, including clathrin-associated adaptor protein 1 (AP-1), tail-interacting protein of 47 kDa (TIP47), and phosphofurin acidic cluster-sorting protein 1 (PACS1) (64–66). The mechanisms underlying the retrieval of the IGF-II receptor overlap significantly with those of proteins involved in the intracellular trafficking of APP and BACE1. More importantly, GGA, PACS1, and retromer complex have been implicated in the control of APP processing (63, 67–69).

Newly synthesized APP and BACE1 undergo secretory trafficking to reach the cell surface and then are internalized into endosomes, where BACE is thought to cleave APP in an acidic environment, leading to Aβ production. APP can be retrieved from endosomes back to TGN by binding to a sorting-related receptor with A-type repeats (SORLA) via PACS1, thereby preventing its processing into Aβ peptides (6, 68). The loss of PACS1 expression or deletion of the PACS1 binding site in SORLA results in increased accumulation and processing of APP in the endosomal compartments (70, 71). Like APP, retrograde transport of BACE1 from endosomes to TGN, as observed for the IGF-II receptor, is mediated by binding to GGA proteins and the retromer complex. Dysfunction of the retromer complex not only causes endosomal accumulation of BACE1 but also increases production of APP–CTF-β and soluble APPβ (62, 72). Thus, cellular trafficking of both BACE1 and APP are intimately related to the regulation of Aβ production. Since the retrieval mechanism of the IGF-II receptor from endosomes to TGN overlaps with that of APP and BACE1, it is plausible that changes introduced by overexpression of the IGF-II receptor, such as an increase of APP in lipid rafts, facilitates the processing of APP within endosomal compartments, leading to the increased production of Aβ peptides. Apart from regulating APP processing, IGF-II receptor overexpression decreased the levels of the Aβ degrading enzyme IDE but not those of neprilysin, which also may contribute to an increase in Aβ levels in the conditioned media by prolonging its half-life (71, 73). Although the significance of continued IGF-II receptor overexpression on APP and BACE1 levels as well as APP processing have been validated by receptor siRNA treatment of MS9II cells in the present study, the functional implications of normal levels of the IGF-II receptor on Aβ metabolism remains to be evaluated in future experiments.

Influence of IGF-II receptor overexpression on lipid raft and Aβ production. Lipid rafts are highly dynamic assemblies of cholesterol and sphingolipids on cellular membranes that have been implicated in a variety of functions, including cellular signaling, lipid and protein sorting, and regulated proteolysis (74–76). Several lines of evidence have implicated lipid raft microdomains in the amyloidogenic processing of APP, while nonamyloidogenic processing occurs mainly in the phospholipid-rich regions outside the raft microdomains (40, 41, 43, 77, 78). Our data show that IGF-II receptor overexpression not only elevated the levels of raft-associated glycosphingolipid GM1 and caveolin 1 but also enhanced CTXB binding at the plasma membrane and its endocytosis via a raft-mediated mechanism. Considering that APP, Aβ, and secretases that generate Aβ are associated with lipid raft domains (79, 80), it is likely that alterations in the levels of raft-associated lipids and proteins affect raft targeting of APP and/or its processing enzymes, leading to altered levels of Aβ production. Indeed, we found increased levels of APP, BACE1, and APP-CTFs in both lipid rafts and nonraft fractions isolated from MS9II cells compared to levels in MS cells. Additionally, the relative raft distribution of full-length APP also was markedly higher in MSII cells. Thus, it is likely that IGF-II receptor overexpression partly enhances Aβ production in MS9II cells by increasing the components of lipid rafts and possibly shifting more APP to raft microdomains of the membranes.

IGF-II receptor, Aβ peptides, and cell viability. Several earlier studies have shown that the increased production and accumulation of APP–CTF-β and Aβ can trigger the loss of neurons/cells or increase their susceptibility to a variety of toxic agents (47, 48, 81). The IGF-II receptor, under certain conditions, also has been shown to regulate cell viability (29, 82–84). However, the functional relationship, if any, between Aβ peptides and the IGF-II receptor in regulating cell viability remains unclear. Our results show that receptor overexpression not only enhances the production and levels of APP–CTF-β and Aβ peptides but also renders the cells more vulnerable to staurosporine-induced toxicity, which partly involves oxidative stress (85–87). Since Aβ can induce the generation of toxic free radicals (88, 89), it is likely that staurosporine toxicity is mediated, at least in part, by increased levels of APP–CTF-β and/or Aβ peptides. This notion is supported by two distinct lines of evidence: (i) inhibition of β-secretase significantly protected MS9II cells from staurosporine-induced toxicity, along with the decreased secretion of Aβ peptides into the conditioned media, and (ii) the finding that the overexpression of mutant *PSEN2*, which triggers Aβ production and the development of an early-onset form of AD, increases neuronal susceptibility to staurosporine-induced toxicity (90). Thus, it would be of interest to determine whether increased Aβ production in familial AD with PS mutations is associated with enhanced levels of the IGF-II receptor observed in the cortical region of the brain (24). Collectively, these results highlight not only the significance of IGF-II receptor overexpression in regulating Aβ production by increasing the levels/processing of APP but also its implications in the loss of cells and contribution to AD pathology.

ACKNOWLEDGMENTS

We thank C. Scott (Kolling Institute of Medical Research, NSW, Australia) for the anti-IGF-II receptor antibody. We also are grateful to Michelle Montgomery and Tsuneya Ikezu for assistance with the adenovirus work.

S.K., Y.W., and G.T. conceived and designed the experiments. Y.W., V.B.-P., and M.E.Z. performed the experiments. Y.W., V.B.-P., M.E.Z., R.G.M., G.T., and S.K. analyzed the data. S.K., R.G.M., R.C.B., and G.T. contributed reagents/materials/analysis tools. Y.W., S.K., G.T., and R.G.M. wrote the paper.

This work was supported by grants from the Natural Sciences and Engineering Research Council of Canada (203518) and Canadian Institutes of Health Research (MOP-84480) to S.K., R01AG019070 grant from National Institutes on Aging (G.T.) and CIHR (MOPC133518) to R.C.B., and National Cancer Institute grant CA91885 to R.M. Y.W. is a recipient of doctoral awards from the Alzheimer Society of Canada and a graduate studentship award from Alberta Innovates-Health Solutions. V.B.-P. is supported by the BrightFocus Foundation Alzheimer's disease research award. Confocal imaging was performed at the Integrated Microscopy Core Facility at the University of Chicago (supported by S10OD010649), and flow cytometry was performed at the University of Chicago Flow Cytometry Core Facility. M.Z. is a recipient of a Davies Fellowship from the University of Nebraska Medical Center.

REFERENCES

1. **Bertram L, Tanzi RE.** 2012. The genetics of Alzheimer's disease. Prog Mol Biol Transl Sci **107:**79–100. http://dx.doi.org/10.1016/B978-0-12-385883-2.00008-4.
2. **Selkoe DJ.** 2011. Alzheimer's disease. Cold Spring Harb Perspect Biol **3:**a004457. http://dx.doi.org/10.1101/cshperspect.a004457.
3. **Karch CM, Cruchaga C, Goate AM.** 2014. Alzheimer's disease genetics: from the bench to the clinic. Neuron **83:**11–26. http://dx.doi.org/10.1016/j.neuron.2014.05.041.
4. **Nelson PT, Braak H, Markesbery WR.** 2009. Neuropathology and cognitive impairment in Alzheimer disease: a complex but coherent relationship. J Neuropathol Exp Neurol **68:**1–14. http://dx.doi.org/10.1097/NEN.0b013e3181919a48.
5. **Thinakaran G, Koo EH.** 2008. Amyloid precursor protein trafficking, processing, and function. J Biol Chem **283:**29615–29619. http://dx.doi.org/10.1074/jbc.R800019200.
6. **Haass C, Kaether C, Thinakaran G, Sisodia S.** 2012. Trafficking and proteolytic processing of APP. Cold Spring Harb Perspect Med **2:**a006270. http://dx.doi.org/10.1101/cshperspect.a006270.
7. **Ghosh P, Dahms NM, Kornfeld S.** 2003. Mannose 6-phosphate receptors: new twists in the tale. Nat Rev Mol Cell Biol **4:**202–212. http://dx.doi.org/10.1038/nrm1050.
8. **Hawkes C, Kar S.** 2004. The insulin-like growth factor-II/mannose-6-phosphate receptor: structure, distribution and function in the central nervous system. Brain Res Brain Res Rev **44:**117–140. http://dx.doi.org/10.1016/j.brainresrev.2003.11.002.
9. **El-Shewy HM, Luttrell LM.** 2009. Insulin-like growth factor-2/mannose-6 phosphate receptors. Vitam Horm **80:**667–697. http://dx.doi.org/10.1016/S0083-6729(08)00624-9.
10. **Kar S, Seto D, Dore S, Hanisch U, Quirion R.** 1997. Insulin-like growth factors-I and -II differentially regulate endogenous acetylcholine release from the rat hippocampal formation. Proc Natl Acad Sci U S A **94:**14054–14059. http://dx.doi.org/10.1073/pnas.94.25.14054.
11. **Dikkes P, Hawkes C, Kar S, Lopez MF.** 2007. Effect of kainic acid treatment on insulin-like growth factor-2 receptors in the IGF2-deficient adult mouse brain. Brain Res **1131:**77–87. http://dx.doi.org/10.1016/j.brainres.2006.11.022.
12. **Couce ME, Weatherington AJ, McGinty JF.** 1992. Expression of insulin-like growth factor-II (IGF-II) and IGF-II/mannose-6-phosphate receptor in the rat hippocampus: an in situ hybridization and immunocytochemical study. Endocrinology **131:**1636–1642. http://dx.doi.org/10.1210/en.131.4.1636.
13. **Kar S, Chabot JG, Quirion R.** 1993. Quantitative autoradiographic localization of [125I]insulin-like growth factor I, [125I]insulin-like growth factor II, and [125I]insulin receptor binding sites in developing and adult rat brain. J Comp Neurol **333:**375–397. http://dx.doi.org/10.1002/cne.903330306.
14. **Kar S, Baccichet A, Quirion R, Poirier J.** 1993. Entorhinal cortex lesion induces differential responses in [125I]insulin-like growth factor I, [125I]insulin-like growth factor II and [125I]insulin receptor binding sites in the rat hippocampal formation. Neuroscience **55:**69–80. http://dx.doi.org/10.1016/0306-4522(93)90455-O.
15. **Stephenson DT, Rash K, Clemens JA.** 1995. Increase in insulin-like growth factor II receptor within ischemic neurons following focal cerebral infarction. J Cereb Blood Flow Metab **15:**1022–1031. http://dx.doi.org/10.1038/jcbfm.1995.128.
16. **Breese CR, D'Costa A, Rollins YD, Adams C, Booze RM, Sonntag WE, Leonard S.** 1996. Expression of insulin-like growth factor-1 (IGF-1) and IGF-binding protein 2 (IGF-BP2) in the hippocampus following cytotoxic lesion of the dentate gyrus. J Comp Neurol **369:**388–404.
17. **Walter HJ, Berry M, Hill DJ, Cwyfan-Hughes S, Holly JM, Logan A.** 1999. Distinct sites of insulin-like growth factor (IGF)-II expression and localization in lesioned rat brain: possible roles of IGF binding proteins (IGFBPs) in the mediation of IGF-II activity. Endocrinology **140:**520–532.
18. **Hawkes C, Kar S.** 2003. Insulin-like growth factor-II/mannose-6-phosphate receptor: widespread distribution in neurons of the central nervous system including those expressing cholinergic phenotype. J Comp Neurol **458:**113–127. http://dx.doi.org/10.1002/cne.10578.
19. **Hawkes C, Kabogo D, Amritraj A, Kar S.** 2006. Up-regulation of cation-independent mannose 6-phosphate receptor and endosomal-lysosomal markers in surviving neurons after 192-IgG-saporin administrations into the adult rat brain. Am J Pathol **169:**1140–1154. http://dx.doi.org/10.2353/ajpath.2006.051208.
20. **Konishi Y, Fushimi S, Shirabe T.** 2005. Immunohistochemical distribution of cation-dependent mannose 6-phosphate receptors in the mouse central nervous system: comparison with that of cation-independent mannose 6-phophate receptors. Neurosci Lett **378:**7–12. http://dx.doi.org/10.1016/j.neulet.2004.12.067.
21. **Pasternak SH, Callahan JW, Mahuran DJ.** 2004. The role of the endosomal/lysosomal system in amyloid-beta production and the pathophysiology of Alzheimer's disease: reexamining the spatial paradox from a lysosomal perspective. J Alzheimers Dis **6:**53–65.
22. **Nixon RA, Cataldo AM.** 2006. Lysosomal system pathways: genes to neurodegeneration in Alzheimer's disease. J Alzheimers Dis **9:**277–289.
23. **Kar S, Poirier J, Guevara J, Dea D, Hawkes C, Robitaille Y, Quirion R.** 2006. Cellular distribution of insulin-like growth factor-II/mannose-6-phosphate receptor in normal human brain and its alteration in Alzheimer's disease pathology. Neurobiol Aging **27:**199–210. http://dx.doi.org/10.1016/j.neurobiolaging.2005.03.005.
24. **Cataldo AM, Peterhoff CM, Schmidt SD, Terio NB, Duff K, Beard M, Mathews PM, Nixon RA.** 2004. Presenilin mutations in familial Alzheimer disease and transgenic mouse models accelerate neuronal lysosomal pathology. J Neuropathol Exp Neurol **63:**821–830.
25. **Amritraj A, Hawkes C, Phinney AL, Mount HT, Scott CD, Westaway D, Kar S.** 2009. Altered levels and distribution of IGF-II/M6P receptor and lysosomal enzymes in mutant APP and APP + PS1 transgenic mouse brains. Neurobiol Aging **30:**54–70. http://dx.doi.org/10.1016/j.neurobiolaging.2007.05.004.
26. **Watanabe H, Grubb JH, Sly WS.** 1990. The overexpressed human 46-kDa mannose 6-phosphate receptor mediates endocytosis and sorting of beta-glucuronidase. Proc Natl Acad Sci U S A **87:**8036–8040. http://dx.doi.org/10.1073/pnas.87.20.8036.
27. **Nolan CM, Kyle JW, Watanabe H, Sly WS.** 1990. Binding of insulin-like growth factor II (IGF-II) by human cation-independent mannose 6-phosphate receptor/IGF-II receptor expressed in receptor-deficient mouse L cells. Cell Regul **1:**197–213.
28. **Wood RJ, Hulett MD.** 2008. Cell surface-expressed cation-independent mannose 6-phosphate receptor (CD222) binds enzymatically active heparanase independently of mannose 6-phosphate to promote extracellular matrix degradation. J Biol Chem **283:**4165–4176. http://dx.doi.org/10.1074/jbc.M708723200.
29. **Motyka B, Korbutt G, Pinkoski MJ, Heibein JA, Caputo A, Hobman M, Barry M, Shostak I, Sawchuk T, Holmes CF, Gauldie J, Bleackley RC.** 2000. Mannose 6-phosphate/insulin-like growth factor II receptor is a death receptor for granzyme B during cytotoxic T cell-induced apoptosis. Cell **103:**491–500. http://dx.doi.org/10.1016/S0092-8674(00)00140-9.
30. **Di Bacco A, Gill G.** 2003. The secreted glycoprotein CREG inhibits cell growth dependent on the mannose-6-phosphate/insulin-like growth fac-

tor II receptor. Oncogene **22:**5436–5445. http://dx.doi.org/10.1038/sj.onc.1206670.
31. **Oshima A, Nolan CM, Kyle JW, Grubb JH, Sly WS.** 1988. The human cation-independent mannose 6-phosphate receptor. Cloning and sequence of the full-length cDNA and expression of functional receptor in COS cells. J Biol Chem **263:**2553–2562.
32. **Dutta D, Williamson CD, Cole NB, Donaldson JG.** 2012. Pitstop 2 is a potent inhibitor of clathrin-independent endocytosis. PLoS One **7:**e45799. http://dx.doi.org/10.1371/journal.pone.0045799.
33. **Amritraj A, Wang Y, Revett TJ, Vergote D, Westaway D, Kar S.** 2013. Role of cathepsin D in U18666A-induced neuronal cell death: potential implication in Niemann-Pick type C disease pathogenesis. J Biol Chem **288:**3136–3152. http://dx.doi.org/10.1074/jbc.M112.412460.
34. **Kreiling JL, Montgomery MA, Wheeler JR, Kopanic JL, Connelly CM, Zavorka ME, Allison JL, Macdonald RG.** 2012. Dominant-negative effect of truncated mannose 6-phosphate/insulin-like growth factor II receptor species in cancer. FEBS J **279:**2695–2713. http://dx.doi.org/10.1111/j.1742-4658.2012.08652.x.
35. **Grimm MO, Grimm HS, Tomic I, Beyreuther K, Hartmann T, Bergmann C.** 2008. Independent inhibition of Alzheimer disease beta- and gamma-secretase cleavage by lowered cholesterol levels. J Biol Chem **283:**11302–11311. http://dx.doi.org/10.1074/jbc.M801520200.
36. **Byrd JC, Park JH, Schaffer BS, Garmroudi F, MacDonald RG.** 2000. Dimerization of the insulin-like growth factor II/mannose 6-phosphate receptor. J Biol Chem **275:**18647–18656. http://dx.doi.org/10.1074/jbc.M001273200.
37. **Maulik M, Ghoshal B, Kim J, Wang Y, Yang J, Westaway D, Kar S.** 2012. Mutant human APP exacerbates pathology in a mouse model of NPC and its reversal by a beta-cyclodextrin. Hum Mol Genet **21:**4857–4875. http://dx.doi.org/10.1093/hmg/dds322.
38. **Wang Y, Thinakaran G, Kar S.** 2014. Overexpression of the IGF-II/M6P receptor in mouse fibroblast cell lines differentially alters expression profiles of genes involved in Alzheimer's disease-related pathology. PLoS One **9:**e98057. http://dx.doi.org/10.1371/journal.pone.0098057.
39. **Hawkes C, Jhamandas JH, Harris KH, Fu W, MacDonald RG, Kar S.** 2006. Single transmembrane domain insulin-like growth factor-II/mannose-6-phosphate receptor regulates central cholinergic function by activating a G-protein-sensitive, protein kinase C-dependent pathway. J Neurosci **26:**585–596. http://dx.doi.org/10.1523/JNEUROSCI.2730-05.2006.
40. **Kojro E, Gimpl G, Lammich S, Marz W, Fahrenholz F.** 2001. Low cholesterol stimulates the nonamyloidogenic pathway by its effect on the alpha-secretase ADAM 10. Proc Natl Acad Sci U S A **98:**5815–5820. http://dx.doi.org/10.1073/pnas.081612998.
41. **Vetrivel KS, Cheng H, Lin W, Sakurai T, Li T, Nukina N, Wong PC, Xu H, Thinakaran G.** 2004. Association of gamma-secretase with lipid rafts in post-Golgi and endosome membranes. J Biol Chem **279:**44945–44954. http://dx.doi.org/10.1074/jbc.M407986200.
42. **Wahrle S, Das P, Nyborg AC, McLendon C, Shoji M, Kawarabayashi T, Younkin LH, Younkin SG, Golde TE.** 2002. Cholesterol-dependent gamma-secretase activity in buoyant cholesterol-rich membrane microdomains. Neurobiol Dis **9:**11–23. http://dx.doi.org/10.1006/nbdi.2001.0470.
43. **Ehehalt R, Keller P, Haass C, Thiele C, Simons K.** 2003. Amyloidogenic processing of the Alzheimer beta-amyloid precursor protein depends on lipid rafts. J Cell Biol **160:**113–123. http://dx.doi.org/10.1083/jcb.200207113.
44. **Cheng H, Vetrivel KS, Gong P, Meckler X, Parent A, Thinakaran G.** 2007. Mechanisms of disease: new therapeutic strategies for Alzheimer's disease–targeting APP processing in lipid rafts. Nat Clin Pract Neurol **3:**374–382. http://dx.doi.org/10.1038/ncpneuro0549.
45. **Torgersen ML, Skretting G, van Deurs B, Sandvig K.** 2001. Internalization of cholera toxin by different endocytic mechanisms. J Cell Sci **114:**3737–3747.
46. **Le PU, Nabi IR.** 2003. Distinct caveolae-mediated endocytic pathways target the Golgi apparatus and the endoplasmic reticulum. J Cell Sci **116:**1059–1071. http://dx.doi.org/10.1242/jcs.00327.
47. **Berger-Sweeney J, McPhie DL, Arters JA, Greenan J, Oster-Granite ML, Neve RL.** 1999. Impairments in learning and memory accompanied by neurodegeneration in mice transgenic for the carboxyl-terminus of the amyloid precursor protein. Brain Res Mol Brain Res **66:**150–162. http://dx.doi.org/10.1016/S0169-328X(99)00014-5.
48. **McPhie DL, Golde T, Eckman CB, Yager D, Brant JB, Neve RL.** 2001. Beta-secretase cleavage of the amyloid precursor protein mediates neuronal apoptosis caused by familial Alzheimer's disease mutations. Brain Res Mol Brain Res **97:**103–113. http://dx.doi.org/10.1016/S0169-328X(01)00294-7.
49. **Herbert JM, Seban E, Maffrand JP.** 1990. Characterization of specific binding sites for [3H]-staurosporine on various protein kinases. Biochem Biophys Res Commun **171:**189–195. http://dx.doi.org/10.1016/0006-291X(90)91375-3.
50. **Ruegg UT, Burgess GM.** 1989. Staurosporine, K-252 and UCN-01: potent but nonspecific inhibitors of protein kinases. Trends Pharmacol Sci **10:**218–220. http://dx.doi.org/10.1016/0165-6147(89)90263-0.
51. **Thinakaran G, Borchelt DR, Lee MK, Slunt HH, Spitzer L, Kim G, Ratovitsky T, Davenport F, Nordstedt C, Seeger M, Hardy J, Levey AI, Gandy SE, Jenkins NA, Copeland NG, Price DL, Sisodia SS.** 1996. Endoproteolysis of presenilin 1 and accumulation of processed derivatives in vivo. Neuron **17:**181–190. http://dx.doi.org/10.1016/S0896-6273(00)80291-3.
52. **Thinakaran G, Harris CL, Ratovitski T, Davenport F, Slunt HH, Price DL, Borchelt DR, Sisodia SS.** 1997. Evidence that levels of presenilins (PS1 and PS2) are coordinately regulated by competition for limiting cellular factors. J Biol Chem **272:**28415–28422. http://dx.doi.org/10.1074/jbc.272.45.28415.
53. **Takasugi N, Tomita T, Hayashi I, Tsuruoka M, Niimura M, Takahashi Y, Thinakaran G, Iwatsubo T.** 2003. The role of presenilin cofactors in the gamma-secretase complex. Nature **422:**438–441. http://dx.doi.org/10.1038/nature01506.
54. **Miners JS, Baig S, Palmer J, Palmer LE, Kehoe PG, Love S.** 2008. Abeta-degrading enzymes in Alzheimer's disease. Brain Pathol **18:**240–252. http://dx.doi.org/10.1111/j.1750-3639.2008.00132.x.
55. **Saido T, Leissring MA.** 2012. Proteolytic degradation of amyloid beta-protein. Cold Spring Harb Perspect Med **2:**a006379. http://dx.doi.org/10.1101/cshperspect.a006379.
56. **Maulik M, Westaway D, Jhamandas JH, Kar S.** 2013. Role of cholesterol in APP metabolism and its significance in Alzheimer's disease pathogenesis. Mol Neurobiol **47:**37–63. http://dx.doi.org/10.1007/s12035-012-8337-y.
57. **Hemming ML, Elias JE, Gygi SP, Selkoe DJ.** 2009. Identification of beta-secretase (BACE1) substrates using quantitative proteomics. PLoS One **4:**e8477. http://dx.doi.org/10.1371/journal.pone.0008477.
58. **Haque A, Banik NL, Ray SK.** 2008. New insights into the roles of endolysosomal cathepsins in the pathogenesis of Alzheimer's disease: cathepsin inhibitors as potential therapeutics. CNS Neurol Disord Drug Targets **7:**270–277. http://dx.doi.org/10.2174/187152708784936653.
59. **Yamashima T.** 2013. Reconsider Alzheimer's disease by the "calpain-cathepsin hypothesis"–a perspective review. Prog Neurobiol **105:**1–23. http://dx.doi.org/10.1016/j.pneurobio.2013.02.004.
60. **Mathews PM, Guerra CB, Jiang Y, Grbovic OM, Kao BH, Schmidt SD, Dinakar R, Mercken M, Hille-Rehfeld A, Rohrer J, Mehta P, Cataldo AM, Nixon RA.** 2002. Alzheimer's disease-related overexpression of the cation-dependent mannose 6-phosphate receptor increases Abeta secretion: role for altered lysosomal hydrolase distribution in beta-amyloidogenesis. J Biol Chem **277:**5299–5307. http://dx.doi.org/10.1074/jbc.M108161200.
61. **Ghosh P, Griffith J, Geuze HJ, Kornfeld S.** 2003. Mammalian GGAs act together to sort mannose 6-phosphate receptors. J Cell Biol **163:**755–766. http://dx.doi.org/10.1083/jcb.200308038.
62. **He X, Li F, Chang WP, Tang J.** 2005. GGA proteins mediate the recycling pathway of memapsin 2 (BACE). J Biol Chem **280:**11696–11703. http://dx.doi.org/10.1074/jbc.M411296200.
63. **Wahle T, Prager K, Raffler N, Haass C, Famulok M, Walter J.** 2005. GGA proteins regulate retrograde transport of BACE1 from endosomes to the trans-Golgi network. Mol Cell Neurosci **29:**453–461. http://dx.doi.org/10.1016/j.mcn.2005.03.014.
64. **Arighi CN, Hartnell LM, Aguilar RC, Haft CR, Bonifacino JS.** 2004. Role of the mammalian retromer in sorting of the cation-independent mannose 6-phosphate receptor. J Cell Biol **165:**123–133. http://dx.doi.org/10.1083/jcb.200312055.
65. **Seaman MN.** 2005. Recycle your receptors with retromer. Trends Cell Biol **15:**68–75. http://dx.doi.org/10.1016/j.tcb.2004.12.004.
66. **McGough IJ, Cullen PJ.** 2011. Recent advances in retromer biology. Traffic **12:**963–971. http://dx.doi.org/10.1111/j.1600-0854.2011.01201.x.
67. **Siegenthaler BM, Rajendran L.** 2012. Retromers in Alzheimer's disease. Neurodegener Dis **10:**116–121. http://dx.doi.org/10.1159/000335910.

68. **Buggia-Prevot V, Thinakaran G.** 2014. Sorting the role of SORLA in Alzheimer's disease. Sci Transl Med **6:**223–228. http://dx.doi.org/10.1126/scitranslmed.3008562.
69. **Jiang S, Li Y, Zhang X, Bu G, Xu H, Zhang YW.** 2014. Trafficking regulation of proteins in Alzheimer's disease. Mol Neurodegener **9:**6. http://dx.doi.org/10.1186/1750-1326-9-6.
70. **Schmidt V, Sporbert A, Rohe M, Reimer T, Rehm A, Andersen OM, Willnow TE.** 2007. SorLA/LR11 regulates processing of amyloid precursor protein via interaction with adaptors GGA and PACS-1. J Biol Chem **282:**32956–32964. http://dx.doi.org/10.1074/jbc.M705073200.
71. **Burgert T, Schmidt V, Caglayan S, Lin F, Fuchtbauer A, Fuchtbauer EM, Nykjaer A, Carlo AS, Willnow TE.** 2013. SORLA-dependent and -independent functions for PACS1 in control of amyloidogenic processes. Mol Cell Biol **33:**4308–4320. http://dx.doi.org/10.1128/MCB.00628-13.
72. **Okada H, Zhang W, Peterhoff C, Hwang JC, Nixon RA, Ryu SH, Kim TW.** 2010. Proteomic identification of sorting nexin 6 as a negative regulator of BACE1-mediated APP processing. FASEB J **24:**2783–2794. http://dx.doi.org/10.1096/fj.09-146357.
73. **Vekrellis K, Ye Z, Qiu WQ, Walsh D, Hartley D, Chesneau V, Rosner MR, Selkoe DJ.** 2000. Neurons regulate extracellular levels of amyloid beta-protein via proteolysis by insulin-degrading enzyme. J Neurosci **20:**1657–1665.
74. **Simons K, Ehehalt R.** 2002. Cholesterol, lipid rafts, and disease. J Clin Investig **110:**597–603. http://dx.doi.org/10.1172/JCI16390.
75. **Jacobson K, Mouritsen OG, Anderson RG.** 2007. Lipid rafts: at a crossroad between cell biology and physics. Nat Cell Biol **9:**7–14. http://dx.doi.org/10.1038/ncb0107-7.
76. **Lingwood D, Simons K.** 2010. Lipid rafts as a membrane-organizing principle. Science **327:**46–50. http://dx.doi.org/10.1126/science.1174621.
77. **Riddell DR, Christie G, Hussain I, Dingwall C.** 2001. Compartmentalization of beta-secretase (Asp2) into low-buoyant density, noncaveolar lipid rafts. Curr Biol **11:**1288–1293. http://dx.doi.org/10.1016/S0960-9822(01)00394-3.
78. **Vetrivel KS, Cheng H, Kim SH, Chen Y, Barnes NY, Parent AT, Sisodia SS, Thinakaran G.** 2005. Spatial segregation of gamma-secretase and substrates in distinct membrane domains. J Biol Chem **280:**25892–25900. http://dx.doi.org/10.1074/jbc.M503570200.
79. **Lee SJ, Liyanage U, Bickel PE, Xia W, Lansbury PT, Jr, Kosik KS.** 1998. A detergent-insoluble membrane compartment contains A beta in vivo. Nat Med **4:**730–734. http://dx.doi.org/10.1038/nm0698-730.
80. **Vetrivel KS, Thinakaran G.** 2010. Membrane rafts in Alzheimer's disease beta-amyloid production. Biochim Biophys Acta **1801:**860–867. http://dx.doi.org/10.1016/j.bbalip.2010.03.007.
81. **Wirths O, Multhaup G, Bayer TA.** 2004. A modified beta-amyloid hypothesis: intraneuronal accumulation of the beta-amyloid peptide–the first step of a fatal cascade. J Neurochem **91:**513–520. http://dx.doi.org/10.1111/j.1471-4159.2004.02737.x.
82. **Li Y, Xu C, Schubert D.** 1999. The up-regulation of endosomal-lysosomal components in amyloid beta-resistant cells. J Neurochem **73:**1477–1482.
83. **Zhou G, Roizman B.** 2002. Cation-independent mannose 6-phosphate receptor blocks apoptosis induced by herpes simplex virus 1 mutants lacking glycoprotein D and is likely the target of antiapoptotic activity of the glycoprotein. J Virol **76:**6197–6204. http://dx.doi.org/10.1128/JVI.76.12.6197-6204.2002.
84. **Weng YS, Kuo WW, Lin YM, Kuo CH, Tzang BS, Tsai FJ, Tsai CH, Lin JA, Hsieh DJ, Huang CY.** 2013. Danshen mediates through estrogen receptors to activate Akt and inhibit apoptosis effect of Leu27IGF-II-induced IGF-II receptor signaling activation in cardiomyoblasts. Food Chem Toxicol **56:**28–39. http://dx.doi.org/10.1016/j.fct.2013.01.008.
85. **Gil J, Almeida S, Oliveira CR, Rego AC.** 2003. Cytosolic and mitochondrial ROS in staurosporine-induced retinal cell apoptosis. Free Radic Biol Med **35:**1500–1514. http://dx.doi.org/10.1016/j.freeradbiomed.2003.08.022.
86. **Pong K, Doctrow SR, Huffman K, Adinolfi CA, Baudry M.** 2001. Attenuation of staurosporine-induced apoptosis, oxidative stress, and mitochondrial dysfunction by synthetic superoxide dismutase and catalase mimetics, in cultured cortical neurons. Exp Neurol **171:**84–97. http://dx.doi.org/10.1006/exnr.2001.7747.
87. **Kruman I, Guo Q, Mattson MP.** 1998. Calcium and reactive oxygen species mediate staurosporine-induced mitochondrial dysfunction and apoptosis in PC12 cells. J Neurosci Res **51:**293–308.
88. **Butterfield DA, Boyd-Kimball D.** 2004. Amyloid beta-peptide(1-42) contributes to the oxidative stress and neurodegeneration found in Alzheimer disease brain. Brain Pathol **14:**426–432. http://dx.doi.org/10.1111/j.1750-3639.2004.tb00087.x.
89. **Cenini G, Cecchi C, Pensalfini A, Bonini SA, Ferrari-Toninelli G, Liguri G, Memo M, Uberti D.** 2010. Generation of reactive oxygen species by beta amyloid fibrils and oligomers involves different intra/extracellular pathways. Amino Acids **38:**1101–1106. http://dx.doi.org/10.1007/s00726-009-0319-7.
90. **Araki W, Yuasa K, Takeda S, Takeda K, Shirotani K, Takahashi K, Tabira T.** 2001. Pro-apoptotic effect of presenilin 2 (PS2) overexpression is associated with down-regulation of Bcl-2 in cultured neurons. J Neurochem **79:**1161–1168. http://dx.doi.org/10.1046/j.1471-4159.2001.00638.x.